

Measurement of the $pp \rightarrow ZZ$ production cross section and constraints on anomalous triple gauge couplings in four-lepton final states at $\sqrt{s} = 8$ TeV

The CMS Collaboration*

Abstract

A measurement of inclusive ZZ production cross section and constraints on anomalous triple gauge couplings in proton-proton collisions at $\sqrt{s} = 8$ TeV are presented. A data sample, corresponding to an integrated luminosity of 19.6 fb^{-1} was collected with the CMS experiment at the LHC. The measurements are performed in the leptonic decay modes $ZZ \rightarrow \ell\ell\ell'\ell'$, where $\ell = e, \mu$ and $\ell' = e, \mu, \tau$. The measured total cross section, $\sigma(pp \rightarrow ZZ) = 7.7 \pm 0.5$ (stat.) $_{-0.4}^{+0.5}$ (syst.) ± 0.4 (th.) ± 0.2 (lum.) pb for both Z bosons produced in the mass range $60 < m_Z < 120$ GeV, is consistent with standard model predictions. Differential cross sections are measured and well described by the theoretical predictions. The invariant mass distribution of the four-lepton system is used to set limits on anomalous ZZZ and $ZZ\gamma$ couplings at the 95% confidence level: $-0.004 < f_4^Z < 0.004$, $-0.005 < f_5^Z < 0.005$, $-0.004 < f_4^\gamma < 0.004$, and $-0.005 < f_5^\gamma < 0.005$.

Submitted to Physics Letters B

1 Introduction

The study of diboson production in proton-proton collisions provides an important test of the non-Abelian structure of the standard model (SM) Lagrangian. In the SM, ZZ production proceeds mainly through quark-antiquark t - and u -channel scattering diagrams. At higher order in QCD gluon-gluon fusion also contributes via box diagrams with quark loops. There are no SM contributions to ZZ production from triple boson vertices, since ZZZ and ZZ γ couplings are not present at tree level. Anomalous triple gauge couplings (ATGC) ZZZ and ZZ γ are introduced using an effective Lagrangian following Ref. [1]. In this parametrization, two ZZZ and two ZZ γ couplings are allowed by electromagnetic gauge invariance and Lorentz invariance for on-shell Z bosons and are parametrized by two CP-violating (f_4^V) and two CP-conserving (f_5^V) parameters, where $V = (Z, \gamma)$. Nonzero ATGC values could be induced by new physics models such as supersymmetry [2].

Previous measurements of the inclusive ZZ cross section by the CMS Collaboration at the LHC were performed in the ZZ $\rightarrow \ell\ell'\ell'\ell'$ decay channels, where $\ell = e, \mu$ and $\ell' = e, \mu, \tau$, with the data corresponding to an integrated luminosity of 5.1 (5.0) fb $^{-1}$ at $\sqrt{s} = 7(8)$ TeV [3, 4]. The measured total cross section, $\sigma(\text{pp} \rightarrow \text{ZZ})$, is $6.24^{+0.86}_{-0.80}$ (stat.) $^{+0.41}_{-0.32}$ (syst.) ± 0.14 (lum.) pb at $\sqrt{s} = 7$ TeV and 8.4 ± 1.0 (stat.) ± 0.7 (syst.) ± 0.4 (lum.) pb at $\sqrt{s} = 8$ TeV for both Z bosons in the mass range $60 < m_Z < 120$ GeV. The ATLAS Collaboration measured 6.7 ± 0.7 (stat.) $^{+0.4}_{-0.3}$ (syst.) ± 0.3 (lum.) pb [5] with a data sample corresponding to an integrated luminosity of 4.6 fb $^{-1}$ at $\sqrt{s} = 7$ TeV and $66 < m_Z < 116$ GeV. Measurements of the ZZ cross sections performed at the Tevatron are summarized in Refs. [6, 7]. All measurements are found to agree with the corresponding SM predictions.

Limits on ZZZ and ZZ γ ATGCs were set by CMS at $\sqrt{s} = 7$ TeV: $-0.011 < f_4^Z < 0.012$, $-0.012 < f_5^Z < 0.012$, $-0.013 < f_4^\gamma < 0.015$, and $-0.014 < f_5^\gamma < 0.014$ at 95% confidence level (CL) [3]. Similar limits were obtained by ATLAS [5].

In this paper, which is based on the full 2012 data set and corresponds to an integrated luminosity of 19.6 fb $^{-1}$, results are presented for the ZZ inclusive and differential production cross sections as well as limits for the ZZZ and ZZ γ ATGCs.

2 The CMS detector and simulation

The CMS detector is described in detail elsewhere [8]; the key components for this analysis are summarized here. The CMS experiment uses a right-handed coordinate system, with the origin at the nominal interaction point, the x axis pointing to the center of the LHC ring, the y axis pointing up (perpendicular to the plane of the LHC ring), and the z axis along the counterclockwise-beam direction. The polar angle θ is measured from the positive z axis and the azimuthal angle ϕ is measured in the x - y plane. The magnitude of the transverse momentum is $p_T = \sqrt{p_x^2 + p_y^2}$. A superconducting solenoid is located in the central region of the CMS detector, providing an axial magnetic field of 3.8 T parallel to the beam direction. The silicon pixel and strip tracker, the crystal electromagnetic calorimeter (ECAL), and the brass and scintillator hadron calorimeter are located within the solenoid and cover the absolute pseudorapidity range $|\eta| < 3.0$, where pseudorapidity is defined as $\eta = -\ln[\tan(\theta/2)]$. The ECAL barrel region (EB) covers $|\eta| < 1.479$ and two endcap regions (EE) cover $1.479 < |\eta| < 3.0$. A quartz-fiber Cherenkov calorimeter extends the coverage up to $|\eta| < 5.0$. Muons are measured in gas ionization detectors embedded in the steel flux-return yoke outside the solenoid. The first level of the CMS trigger system, composed of custom hardware processors, is designed

to select events of interest in less than $4 \mu\text{s}$ using information from the calorimeters and muon detectors. The high-level-trigger processor farm reduces the event rate from 100 kHz delivered by the first level trigger to a few hundred hertz.

Several Monte Carlo (MC) event generators are used to simulate the signal and background contributions. The ZZ production through $q\bar{q}$ annihilation is generated at next-to-leading order (NLO) with POWHEG 2.0 [9–11] or at leading-order (LO) with SHERPA [12]. The $gg \rightarrow ZZ$ process is simulated with GG2ZZ [13] at LO. Other diboson processes ($WZ, Z\gamma$) and the Z+jets samples are generated at LO with MADGRAPH 5 [14]. Events from $t\bar{t}$ production are generated at NLO with POWHEG. The PYTHIA 6.4 [15] package is used for parton showering, hadronization, and the underlying event simulation. For LO generators, the default set of parton distribution functions (PDF) used to produce these samples is CTEQ6L [16], whereas CT10 [17] is used for NLO generators. The ZZ yields from simulation are scaled according to the theoretical value of the cross sections calculated with MCFM 6.0 [18] at NLO for $qq \rightarrow ZZ$ and LO for $gg \rightarrow ZZ$ with the MSTW2008 PDF [19] with renormalization and factorization scales set to $\mu_R = \mu_F = m_Z$. The τ -lepton decays are simulated with TAUOLA [20]. For all processes, the detector response is simulated using a detailed description of the CMS detector based on the GEANT4 package [21], and event reconstruction is performed with the same algorithms that are used for data. The simulated samples include multiple interactions per bunch crossing (pileup), such that the pileup distribution matches that of data, with an average value of about 21 interactions per bunch crossing.

3 Event reconstruction

A complete reconstruction of the individual particles emerging from each collision event is obtained via a particle-flow (PF) technique [22, 23], which uses the information from all CMS sub-detectors to identify and reconstruct individual particles in the collision event. The particles are classified into mutually exclusive categories: charged hadrons, neutral hadrons, photons, muons, and electrons.

Electrons are reconstructed within the geometrical acceptance, $|\eta^e| < 2.5$, and for transverse momentum $p_T^e > 7 \text{ GeV}$. The reconstruction combines the information from clusters of energy deposits in the ECAL and the trajectory in the inner tracker [24]. Particle trajectories in the tracker volume are reconstructed using a modeling of the electron energy loss and fitted with a Gaussian sum filter [25]. The contribution of the ECAL energy deposits to the electron transverse momentum measurement and its uncertainty are determined via a multivariate regression approach. Electron identification relies on a multivariate technique that combines observables sensitive to the amount of bremsstrahlung along the electron trajectory, the geometrical and momentum matching between the electron trajectory and associated clusters, as well as shower shape observables.

Muons are reconstructed within $|\eta^\mu| < 2.4$ and for $p_T^\mu > 5 \text{ GeV}$ [26]. The reconstruction combines information from both the silicon tracker and the muon detectors. The PF muons are selected from among the reconstructed muon track candidates by applying minimal requirements on the track components in the muon system and matching with minimum ionizing particle energy deposits in the calorimeters.

For τ leptons, two principal decay modes are distinguished: a leptonic mode, τ_ℓ , with a final state including either an electron or a muon, and a hadronic mode, τ_h , with a final state including hadrons. The PF particles are used to reconstruct τ_h with the “hadron-plus-strip” algorithm [27], which optimizes the reconstruction and identification of specific τ_h decay modes.

The π^0 components of the τ_h decays are first reconstructed and then combined with charged hadrons to reconstruct the τ_h decay modes. Cases where τ_h includes three charged hadrons are also included. The missing transverse energy that is associated with neutrinos from τ decays is ignored in the reconstruction. The τ_h candidates in this analysis are required to have $|\eta^{\tau_h}| < 2.3$ and $p_T^{\tau_h} > 20$ GeV.

The isolation of individual electrons or muons is measured relative to their transverse momentum p_T^ℓ , by summing over the transverse momenta of charged hadrons and neutral particles in a cone with $\Delta R = \sqrt{(\Delta\eta)^2 + (\Delta\phi)^2} < 0.4$ around the lepton direction at the interaction vertex:

$$R_{\text{Iso}}^\ell = \left(\sum p_T^{\text{charged}} + \text{MAX} \left[0, \sum p_T^{\text{neutral}} + \sum p_T^\gamma - \rho \times A_{\text{eff}} \right] \right) / p_T^\ell. \quad (1)$$

The $\sum p_T^{\text{charged}}$ is the scalar sum of the transverse momenta of charged hadrons originating from the primary vertex. The primary vertex is chosen as the vertex with the highest sum of p_T^2 of its constituent tracks. The $\sum p_T^{\text{neutral}}$ and $\sum p_T^\gamma$ are the scalar sums of the transverse momenta for neutral hadrons and photons, respectively. The average transverse-momentum flow density ρ is calculated in each event using a ‘‘jet area’’ [28], where ρ is defined as the median of the $p_T^{\text{jet}} / A_{\text{jet}}$ distribution for all pileup jets in the event, each of area A_{jet} . The effective area A_{eff} is the geometric area of the isolation cone times an η -dependent correction factor that accounts for the residual dependence of the isolation on pileup. Electrons and muons are considered isolated if $R_{\text{Iso}}^\ell < 0.4$. Allowing τ leptons in the final state increases the background contamination, therefore tighter isolation requirements are imposed for electrons and muons in $ZZ \rightarrow \ell\ell\tau\tau$ decays: $R_{\text{Iso}}^\ell < 0.25$ for $Z \rightarrow \tau_\ell^+ \tau_\ell^-$, and $R_{\text{Iso}}^e < 0.1$ for $Z \rightarrow \tau_e \tau_h$, and $R_{\text{Iso}}^\mu < 0.15$ for $\tau_\mu \tau_h$.

The isolation of the τ_h is calculated as the scalar sum of the transverse momenta of the charged hadrons and neutral particles in a cone of $\Delta R < 0.5$ around the τ_h direction reconstructed at the interaction vertex. The τ_h isolation includes a correction for pileup effects, which is based on the scalar sum of transverse momenta of charged particles not associated with the primary vertex in a cone of $\Delta R < 0.8$ about the τ_h candidate direction (p_T^{PU}). The isolation variable is defined as:

$$I^{\text{PF}} = \left(\sum p_T^{\text{charged}} + \text{MAX} \left[0, \sum p_T^{\text{neutral}} + \sum p_T^\gamma - f \times p_T^{\text{PU}} \right] \right), \quad (2)$$

where the scale factor of $f = 0.0729$, which is used in estimating the contribution to the isolation sum from neutral hadrons and photons, accounts for the difference in the cone sizes. Two standard working points are defined based on the value of the isolation sum corrected for the pileup contribution: $I^{\text{PF}} < 1$ (8) GeV for final states including one (two) τ_h candidates.

The electron and muon pairs from Z-boson decays are required to originate from the primary vertex. This is ensured by demanding that the significance of the three-dimensional impact parameter relative to the event vertex, $\text{SIP}_{3\text{D}}$, satisfies $\text{SIP}_{3\text{D}} = \left| \frac{\text{IP}}{\sigma_{\text{IP}}} \right| < 4$ for each lepton. The IP is the distance of closest approach of the lepton track to the primary vertex and σ_{IP} is its associated uncertainty.

The efficiencies for the product of reconstruction, identification, and isolation of primary electrons or muons are measured in data using a ‘‘tag-and-probe’’ technique [29] applied to an inclusive sample of Z events. The measurements are performed in bins of p_T^ℓ and $|\eta^\ell|$. The efficiency for selecting electrons in the ECAL barrel(endcaps) is about 70%(60%) for $7 < p_T^e < 10$ GeV, 85%(77%) at $p_T^e \simeq 10$ GeV, and 95%(89%) for $p_T^e \geq 20$ GeV. It is about 85% in the transition region between the ECAL barrel and endcaps ($1.44 < |\eta| < 1.57$), averaging over the whole p_T range. The muons are reconstructed and identified with an efficiency greater than $\sim 98\%$ in the full $|\eta^\mu| < 2.4$ range. The τ_h reconstruction efficiency is approximately 50% [27].

Final-state radiation (FSR) may affect the measured four-momentum of the leptons if it is not properly included in the reconstruction. For electrons, a significant portion of the FSR photons is included in the reconstructed energy because of the size of the electromagnetic clusters, but for muons additional treatment of the FSR photons is important. All photons reconstructed within $|\eta^\mu| < 2.4$ are considered as possible FSR candidates if they have a transverse momentum $p_T^\gamma > 2(4)$ GeV and are found within $\Delta R < 0.07(0.07 < \Delta R < 0.5)$ from the closest selected lepton candidate and are isolated. The photon isolation observable R_{Iso}^γ is the sum, divided by p_T^γ , of the transverse momenta of charged hadrons, neutral hadrons, and photons in a cone of $\Delta R < 0.3$ around the candidate photon direction. Isolated photons must satisfy $R_{\text{Iso}}^\gamma < 1$. The recovered FSR photon is included in the lepton four-momentum and the lepton isolation is then recalculated without it.

The performance of the FSR selection algorithm has been determined using simulated samples, and the rate is verified with the Z and ZZ events in data. The photons within the acceptance for the FSR selection are reconstructed with an efficiency of about 50% and with a mean purity of 80%. The FSR photons are recovered in 0.5(5)% of inclusive Z events with electron (muon) pairs.

4 Event selection

Potential ZZ events are first selected by the trigger system, which requires the presence of a pair of electrons or muons, or a triplet of electrons. Triggers requiring an electron and a muon are also used. For the double-lepton triggers, the highest p_T and second highest p_T leptons are required to exceed 17 and 8 GeV, respectively, while for the triple-electron trigger the thresholds are 15, 8, and 5 GeV. The trigger efficiency for ZZ events within the acceptance of this analysis is greater than 98%.

In selected ZZ events, the Z candidate with the mass closest to the Z-boson mass is denoted Z_1 and the other one, Z_2 . The selection is designed to give mutually exclusive sets of signal candidates first selecting ZZ decays to $4e$, 4μ , and $2e2\mu$, in the following denoted $\ell\ell\ell''\ell''$; these events are not considered in $ZZ \rightarrow \ell\ell\tau\tau$ channel. The leptons are identified and isolated as described in Section 3. The significance of the impact parameter with respect to the primary vertex is required to be $\text{SIP}_{3D} < 4$. When building the Z candidates, the FSR photons are kept if $|m_{\ell\ell\gamma} - m_Z| < |m_{\ell\ell} - m_Z|$ and $m_{\ell\ell\gamma} < 100$ GeV. In the following, the presence of the photons in the $\ell\ell\ell''\ell''$ kinematics is implicit. The leptons constituting a Z candidate are required to be the same flavor and to have opposite charges ($\ell^+\ell^-$). The pair is retained if it satisfies $60 < m_Z < 120$ GeV. If more than one Z_2 candidate satisfies all criteria, the ambiguity is resolved by choosing the pair of leptons with the highest scalar sum of p_T . Among the four selected leptons forming the Z_1 and the Z_2 , at least one should have $p_T > 20$ GeV and another one should have $p_T > 10$ GeV. These p_T thresholds ensure that the selected events have leptons with p_T values on the high-efficiency plateau for the trigger.

For the $\ell\ell\tau\tau$ final state, events are required to have one $Z_1 \rightarrow \ell^+\ell^-$ candidate with $p_T > 20$ GeV for one of the leptons and $p_T > 10$ GeV for the other lepton, and a $Z_2 \rightarrow \tau^+\tau^-$, with τ decaying into e , μ , or τ_h . The leptons from the τ_ℓ decays are required to have $p_T^\ell > 10$ GeV. The τ_h candidates are required to have $p_T^{\tau_h} > 20$ GeV. The FSR recovery is not applied to the $\ell\ell\tau\tau$ final states, since it does not improve the mass reconstruction. The invariant mass of the reconstructed Z_1 is required to satisfy $60 < m_{\ell\ell} < 120$ GeV, and that of the Z_2 to satisfy $m_{\text{min}} < m_{\tau\tau} < 90$ GeV, where $m_{\text{min}} = 20$ GeV for $Z_2 \rightarrow \tau_e\tau_\mu$ final states and 30 GeV for all others.

5 Background estimate

The lepton identification and isolation requirements described in Section 3 significantly suppress all background contributions, and the remnant portion of them arise mainly from the Z and WZ production in association with jets, as well as $t\bar{t}$. In all these cases, a jet or a non-isolated lepton is misidentified as an isolated e , μ , τ_h , τ_e , or τ_μ . To estimate the expected number of background events in the signal region, control data samples are defined for each lepton flavor combination $\ell'\ell'$. The e and τ_e , and μ and τ_μ are considered as different flavors, since they originate from different particles.

The control data samples for the background estimate are obtained by selecting events containing Z_1 , which passes all selection requirements, and two additional lepton candidates $\ell'\ell'$. The additional lepton pair must have opposite charge and matching flavor ($e^\pm e^\mp$, $\mu^\pm \mu^\mp$, $\tau^\pm \tau^\mp$). Control data samples enriched with Z+X events, where X stands for $b\bar{b}$, $c\bar{c}$, gluon, or light quark jets, are obtained by requiring that both additional leptons pass only relaxed identification criteria and are not required to be isolated. By requiring one of the additional leptons to pass the full selection requirements, one obtains data samples enriched with WZ events and significant number of $t\bar{t}$ events. The expected number of background events in the signal region for each flavor pair is obtained by scaling the number of observed $Z_1 + \ell'\ell'$ events by the lepton misidentification probability and combining the results for Z+X and WZ, $t\bar{t}$ control regions together. The procedure is identical for all lepton flavors.

The misidentification probability, i.e., the probability for a lepton candidate that passes the relaxed requirements to pass the full selection, is measured separately for each flavor from a sample of $Z_1 + \ell_{\text{candidate}}$ events with a relaxed identification and no isolation requirements on the $\ell_{\text{candidate}}$. The misidentification probability for each lepton flavor is defined as the ratio of the number of leptons that pass the final isolation and identification requirements to the total number of leptons in the sample. It is measured in bins of lepton p_T and η . The contamination from WZ events, which may lead to an overestimate of the misidentification probability because of the presence of genuine isolated leptons, is suppressed by requiring that the measured missing transverse energy is less than 25 GeV.

The estimated background contributions to the signal region are summarized in Table 1. The procedure excludes a possible double counting of events and contains corrections for small contributions of prompt leptons, which may enter the control data sample. The predicted background rate has a small effect on the ZZ cross section measurement in the $\ell\ell'\ell''$ channels, but is comparable to the signal size for the case of $\ell\ell\tau\tau$.

6 Systematic uncertainties

The systematic uncertainties for trigger efficiency (1.5%) are evaluated from data. The uncertainties on the event yield associated with lepton identification and isolation are 1–2% for muons and electrons, and 6–7% for τ_h . The uncertainty in the LHC integrated luminosity of the data sample is 2.6% [30].

Theoretical uncertainties in the $ZZ \rightarrow \ell\ell'\ell''\ell''$ acceptance are evaluated using MCFM and by varying the renormalization and factorization scales, up and down, by a factor of two with respect to the default values $\mu_R = \mu_F = m_Z$. The variations in the acceptance are 0.1% (NLO $q\bar{q} \rightarrow ZZ$) and 0.4% ($gg \rightarrow ZZ$), and can be neglected. Uncertainties related to the choice of the PDF and the strong coupling constant α_s are evaluated following the PDF4LHC [31] prescription and using CT10, MSTW08, and NNPDF [32] PDF sets and found to be 4% (NLO

$q\bar{q} \rightarrow ZZ$) and 5% ($gg \rightarrow ZZ$).

The uncertainties in Z +jets, WZ +jets, and $t\bar{t}$ yields reflect the uncertainties in the measured values of the misidentification rates and the limited statistics of the control regions in the data, and vary between 20 and 70%.

The uncertainty in the unfolding procedure discussed in Section 7 arises from differences between SHERPA and POWHEG for the unfolding factors (2–3%), from scale and PDF uncertainties (4–5%), and from experimental uncertainties (4–5%).

7 The ZZ cross section measurement

The measured and expected event yields for all decay channels are summarized in Table 1. The reconstructed four-lepton invariant mass distributions for the $4e$, 4μ , $2e2\mu$, and summed $\ell\ell\tau\tau$ decay channels are shown in Fig. 1 and compared with the SM expectations. The shape of the background is taken from data. The reconstructed four-lepton invariant mass distribution for the combined $4e$, 4μ , and $2e2\mu$ channels is shown in Fig. 2(upper left). Figure 2(upper right) presents the invariant mass of the Z_1 candidates. Figures 2(lower left) and (lower right) show the correlation between the reconstructed Z_1 and Z_2 masses for (lower left) $4e$, 4μ , and $2e2\mu$ and for (lower right) $\ell\ell\tau\tau$ final states. The data are well reproduced by the signal simulation and with background predictions estimated from data.

Table 1: The expected yields of ZZ and background events, as well as their sum (“Total expected”) are compared with the observed yields for each decay channel. The statistical and systematic uncertainties are also shown.

Decay channel	Expected ZZ yield	Background	Total expected	Observed
$4e$	$55.28 \pm 0.25 \pm 7.64$	$2.16 \pm 0.26 \pm 0.88$	$57.44 \pm 0.37 \pm 7.69$	54
4μ	$77.32 \pm 0.29 \pm 10.08$	$1.19 \pm 0.36 \pm 0.48$	$78.51 \pm 0.49 \pm 10.09$	75
$2e2\mu$	$136.09 \pm 0.59 \pm 17.50$	$2.35 \pm 0.34 \pm 0.93$	$138.44 \pm 0.70 \pm 17.52$	148
$ee\tau_h\tau_h$	$2.46 \pm 0.03 \pm 0.32$	$3.46 \pm 0.34 \pm 1.04$	$5.92 \pm 0.36 \pm 1.15$	10
$\mu\mu\tau_h\tau_h$	$2.80 \pm 0.03 \pm 0.34$	$3.89 \pm 0.37 \pm 1.17$	$6.69 \pm 0.39 \pm 1.30$	10
$ee\tau_e\tau_h$	$2.79 \pm 0.03 \pm 0.36$	$3.87 \pm 1.26 \pm 1.16$	$6.76 \pm 1.34 \pm 1.29$	9
$\mu\mu\tau_e\tau_h$	$2.87 \pm 0.03 \pm 0.37$	$1.49 \pm 0.67 \pm 0.60$	$4.36 \pm 0.71 \pm 0.73$	2
$ee\tau_\mu\tau_h$	$3.27 \pm 0.03 \pm 0.42$	$1.47 \pm 0.41 \pm 0.44$	$4.74 \pm 0.43 \pm 0.63$	2
$\mu\mu\tau_\mu\tau_h$	$3.81 \pm 0.03 \pm 0.50$	$1.55 \pm 0.43 \pm 0.46$	$5.36 \pm 0.46 \pm 0.70$	5
$ee\tau_e\tau_\mu$	$2.23 \pm 0.03 \pm 0.29$	$3.04 \pm 1.32 \pm 1.50$	$5.27 \pm 1.40 \pm 1.61$	4
$\mu\mu\tau_e\tau_\mu$	$2.41 \pm 0.03 \pm 0.32$	$0.74 \pm 0.51 \pm 0.37$	$3.15 \pm 0.54 \pm 0.51$	5
Total $\ell\ell\tau\tau$	$22.65 \pm 0.05 \pm 2.94$	$19.51 \pm 2.15 \pm 5.85$	$42.16 \pm 2.28 \pm 6.87$	47

The measured yields are used to evaluate the total ZZ production cross section. The signal acceptance is evaluated from simulation and corrected for each individual lepton flavor in bins of p_T and η using factors obtained with the “tag-and-probe” technique. The requirements on p_T and η for the particles in the final state reduce the full possible phase space of the $ZZ \rightarrow 4\ell$ measurement by a factor of 0.56–0.59 for the $4e$, 4μ , and $2e2\mu$ and by a factor of 0.18–0.21 for the $\ell\ell\tau\tau$ final states, with respect to all events generated in the mass window $60 < m_{Z_1}, m_{Z_2} < 120$ GeV. The branching fraction for $Z \rightarrow \ell'\ell'$ is $(3.3658 \pm 0.0023)\%$ for each lepton flavor [33].

To include all final states in the cross section calculation, a simultaneous fit to the number of observed events in all decay channels is performed. The likelihood is written as a combination of individual channel likelihoods for the signal and background hypotheses, with statistical

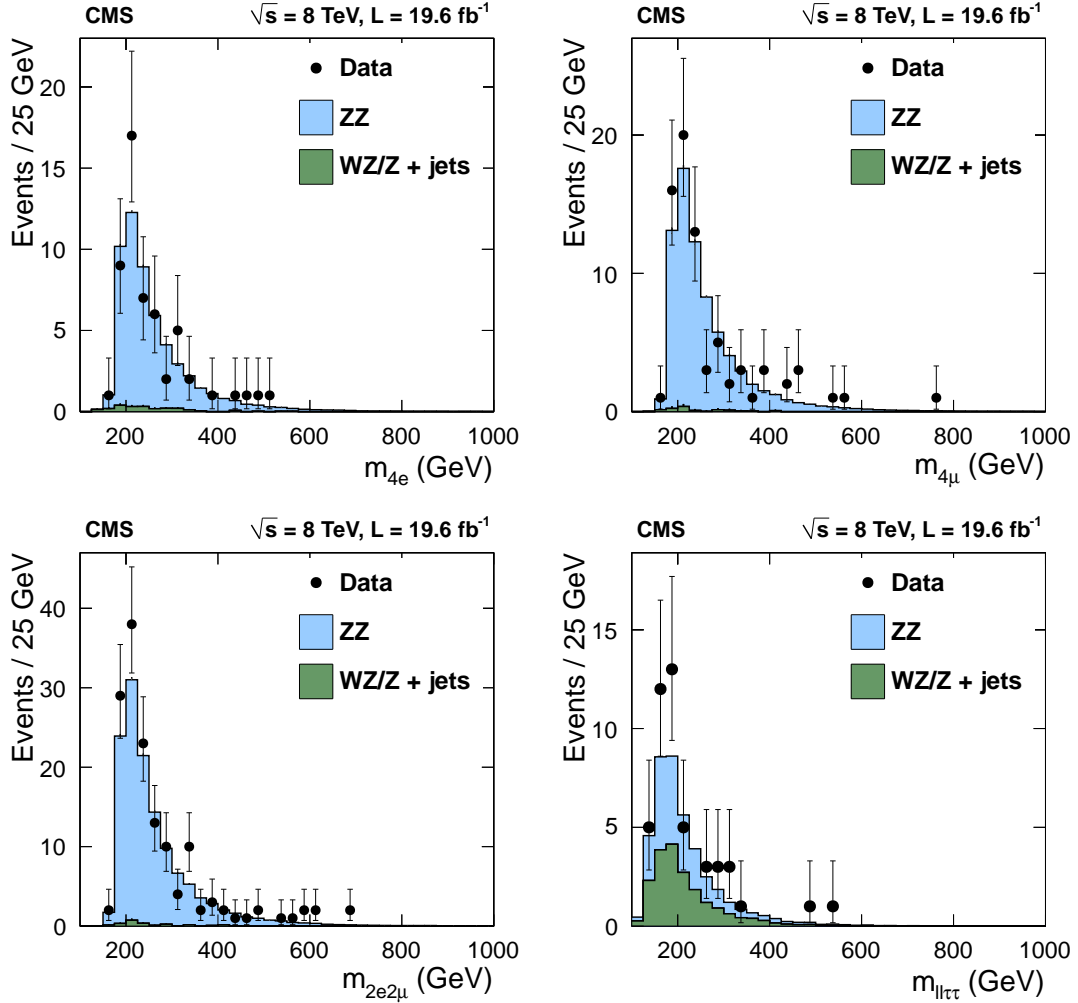


Figure 1: Distribution of the reconstructed four-lepton mass for the (upper left) $4e$, (upper right) 4μ , (lower left) $2e2\mu$, and (lower right) summed $ll\tau\tau$ decay channels. The data sample corresponds to an integrated luminosity of 19.6 fb^{-1} . Points represent the data, the shaded histograms labeled ZZ represent the POWHEG +GG2ZZ+PYTHIA predictions for ZZ signal, the histograms labeled WZ/Z+jets show the background, which is estimated from data, as described in the text.

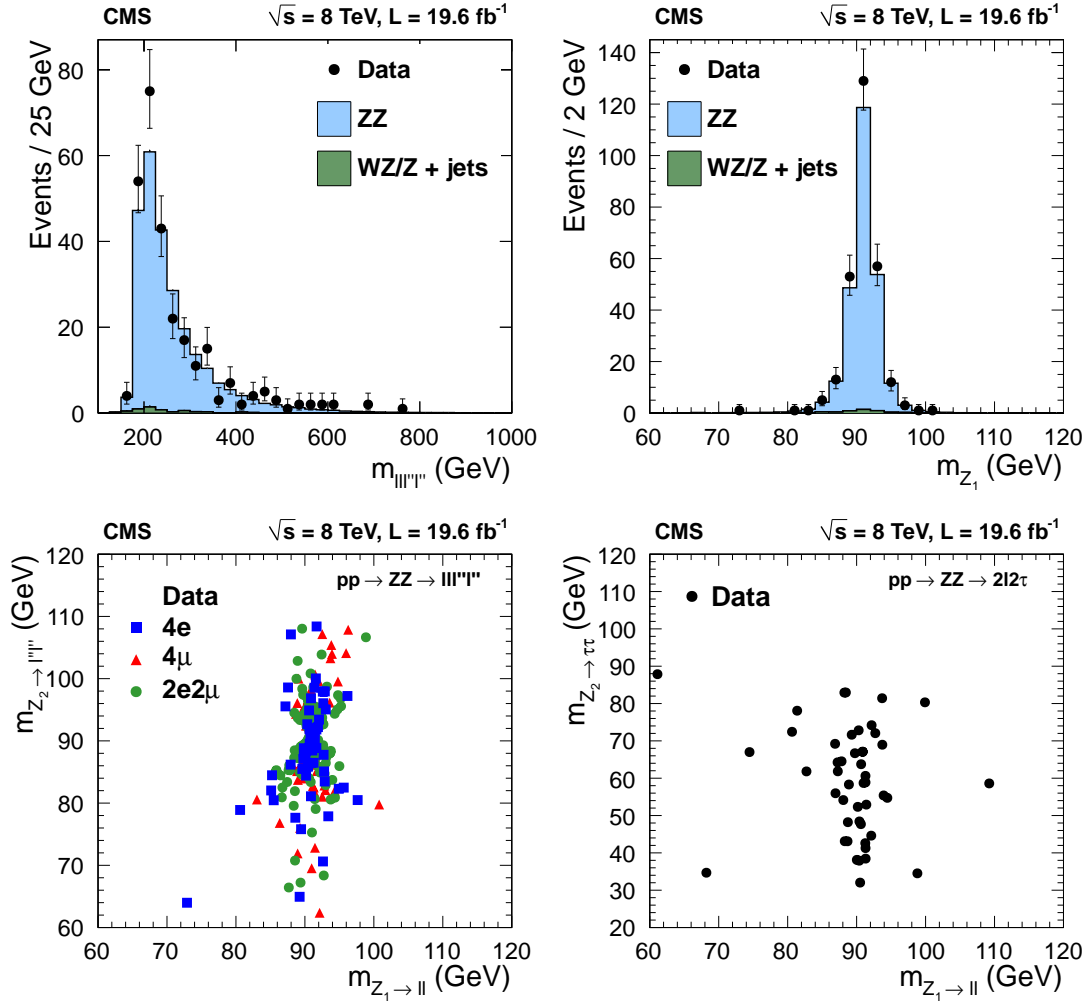


Figure 2: (upper left) Distribution of the reconstructed four-lepton mass for the sum of the 4e, 4μ, and 2e2μ decay channels. (upper right) Reconstructed Z_1 mass. The correlation between the reconstructed Z_1 and Z_2 masses for the (lower left) combined 4e, 4μ, and 2e2μ final states and (lower right) for $ll\tau\tau$ final states. Points represent the data, the shaded histograms labeled ZZ represent the POWHEG +GG2ZZ+PYTHIA predictions for ZZ signal, the histograms labeled WZ/Z+jets show background, which is estimated from data, as described in the text.

and systematical uncertainties used as nuisance parameters in the fit. Each τ -lepton decay mode, listed in Table 1, is treated as a separate channel.

Table 2 lists the total cross section obtained from each individual decay mode as well as the total cross section based on the combination of all channels.

Table 2: The total ZZ production cross section as measured in each decay channel and for the combination of all channels.

Decay channel	Total cross section, pb
4e	$7.2^{+1.0}_{-0.9}$ (stat.) $^{+0.6}_{-0.5}$ (syst.) ± 0.4 (th.) ± 0.2 (lum.)
4 μ	$7.3^{+0.8}_{-0.8}$ (stat.) $^{+0.6}_{-0.5}$ (syst.) ± 0.4 (th.) ± 0.2 (lum.)
2e2 μ	$8.1^{+0.7}_{-0.6}$ (stat.) $^{+0.6}_{-0.5}$ (syst.) ± 0.4 (th.) ± 0.2 (lum.)
$\ell\ell\tau\tau$	$7.7^{+2.1}_{-1.9}$ (stat.) $^{+2.0}_{-1.8}$ (syst.) ± 0.4 (th.) ± 0.2 (lum.)
Combined	7.7 ± 0.5 (stat.) $^{+0.5}_{-0.4}$ (syst.) ± 0.4 (th.) ± 0.2 (lum.)

The measured cross sections can be compared to the theoretical value of 7.7 ± 0.6 pb calculated with MCFM 6.0 at NLO $q\bar{q} \rightarrow ZZ$ and LO $g g \rightarrow ZZ$ with the MSTW2008 PDF and renormalization and factorization scales set to $\mu_R = \mu_F = m_Z$.

The measurement of the differential cross sections is an important part of this analysis, since it provides detailed information about ZZ kinematics. Three decay channels, 4e, 4 μ , and 2e2 μ , are combined, since their kinematic distributions are the same; the $\ell\ell\tau\tau$ channel is not included. The observed yields are unfolded using the method described in Ref. [34].

The differential distributions normalized to the fiducial cross sections are presented in Figs. 3 and 4 for the combination of the 4e, 4 μ , and 2e2 μ decay channels. The fiducial cross section definition includes p_T^ℓ and $|\eta^\ell|$ selections on each lepton, and the 60–120 GeV mass requirement. Figure 3 shows the differential cross sections in bins of p_T for: (upper left) the highest- p_T lepton in the event, (upper right) the Z_1 , and (lower left) the ZZ system. Figure 3(lower left) shows the normalized $d\sigma/dm_{ZZ}$ distribution. The data are corrected for background contributions and compared with the theoretical predictions from POWHEG and MCFM. The bottom part of each plot shows the ratio of the measured to the predicted values. Figure 4 shows the angular correlations between Z bosons, which are in good agreement with the MC simulations. Some difference between POWHEG and MCFM calculations appears at very low p_T of the ZZ system and for azimuthal separation of the Z bosons close to π . This region is better modeled by POWHEG interfaced with the PYTHIA parton shower program.

8 Limits on anomalous triple gauge couplings

The presence of ATGCs would be manifested as an increased yield of events at high four-lepton masses. Figure 5 presents the distribution of the four-lepton reconstructed mass, which is used to set the limits, for the combined 4e, 4 μ , and 2e2 μ channels. The shaded histogram represents the results of the POWHEG simulation for the ZZ signal, and the dashed line, which agrees well with it, is the prediction of SHERPA for $f_4^Z = 0$ normalized to the MCFM cross section. The dotted line indicates the SHERPA predictions for a specific ATGC value ($f_4^Z = 0.015$) with all the other anomalous couplings set to zero.

The invariant mass distributions are interpolated from the SHERPA simulation for different values of the anomalous couplings in the range between 0 and 0.015. For each distribution, only one or two couplings are varied while all others are set to zero. The expected signal is obtained

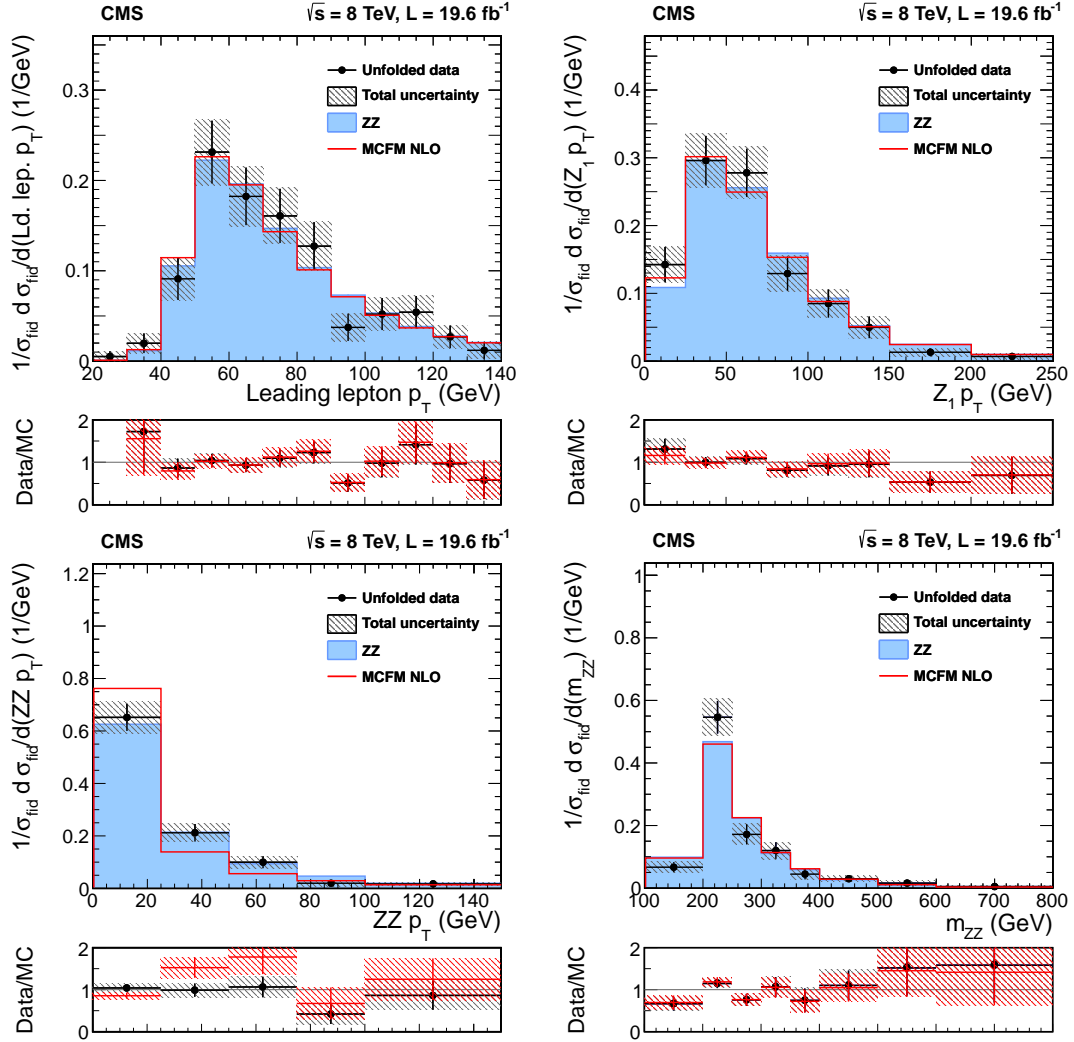


Figure 3: Differential cross sections normalized to the fiducial cross section for the combined $4e$, 4μ , and $2e2\mu$ decay channels as a function of p_T for (upper left) the highest p_T lepton in the event, (upper right) the Z_1 , and (lower left) the ZZ system. Figure (lower right) shows the normalized $d\sigma/dm_{ZZ}$ distribution. Points represent the data, and the shaded histograms labeled ZZ represent the POWHEG +GG2ZZ+PYTHIA predictions for ZZ signal, while the solid curves correspond to results of the MCFM calculations. The bottom part of each subfigure represents the ratio of the measured cross section to the expected one from POWHEG +GG2ZZ+PYTHIA (black crosses with solid symbols) and MCFM (red crosses). The shaded areas on all the plots represent the full uncertainties calculated as the quadrature sum of the statistical and systematic uncertainties, whereas the crosses represent the statistical uncertainties only.

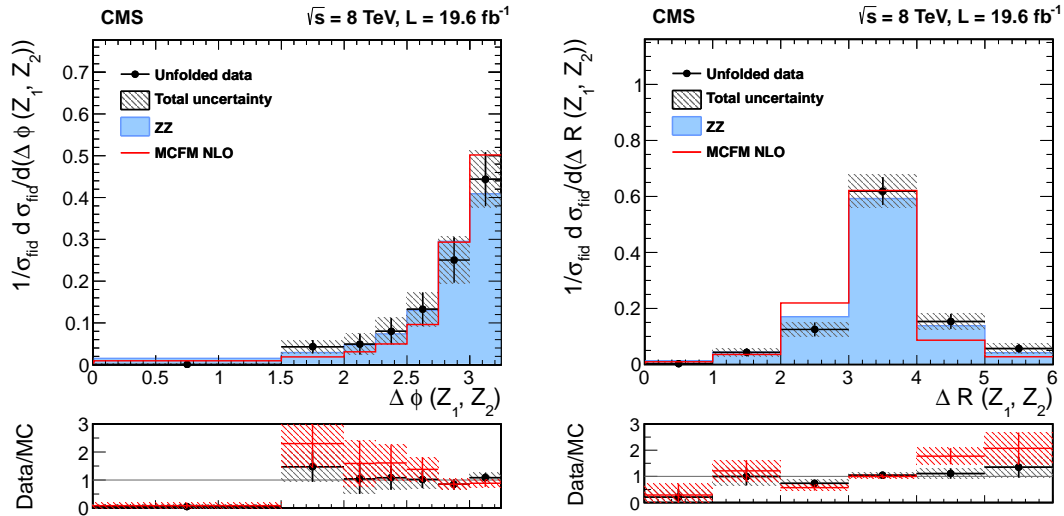


Figure 4: Differential cross section normalized to the fiducial cross section for the combined $4e$, 4μ , and $2e2\mu$ decay channels as a function of (left) azimuthal separation of the two Z bosons and (right) ΔR between the Z -bosons. Points represent the data, and the shaded histograms labeled ZZ represent the POWHEG +GG2ZZ+PYTHIA predictions for ZZ signal, while the solid curves correspond to results of the MCFM calculations. The bottom part of each subfigure represents the ratio of the measured cross section to the expected one from POWHEG +GG2ZZ+PYTHIA (black crosses with solid symbols) and MCFM (red crosses). The shaded areas on all the plots represent the full uncertainties calculated as the quadrature sum of the statistical and systematic uncertainties, whereas the crosses represent the statistical uncertainties only.

from a comparison of the data to a grid of ATGC models in the (f_4^Z, f_4^γ) and (f_5^Z, f_5^γ) parameter planes. Expected signal values are interpolated between the 2D grid points using a second-degree polynomial, since the cross section for signal depends quadratically on the coupling parameters. A profile likelihood method [33] is used to derive the limits. Systematic uncertainties are taken into account by varying the number of expected signal and background events within their uncertainties. No form factor is used when deriving the limits so that the results do not depend on any assumed energy scale characterizing new physics. The constraints on anomalous couplings are displayed in Fig. 6. The curves indicate 68% and 95% confidence levels, and the solid dot shows where the likelihood reaches its maximum. Coupling values outside the contours are excluded at the corresponding confidence levels. The limits are dominated by statistical uncertainties.

One-dimensional 95% CL limits for the $f_4^{Z,\gamma}$ and $f_5^{Z,\gamma}$ anomalous coupling parameters are:

$$-0.004 < f_4^Z < 0.004, \quad -0.005 < f_5^Z < 0.005, \quad -0.004 < f_4^\gamma < 0.004, \quad -0.005 < f_5^\gamma < 0.005.$$

In the one-dimensional fits, all of the ATGC parameters except the one under study are set to zero. These values extend previous CMS results on vector boson self-interactions [3] and improve on the previous limits by factors of three to four, they are presented in Fig. 6 as horizontal and vertical lines.

9 Summary

Measurements have been presented of inclusive ZZ production cross section in proton-proton collisions at 8 TeV in the $ZZ \rightarrow \ell\ell\ell'\ell'$ decay mode, with $\ell = e, \mu$ and $\ell' = e, \mu, \tau$. The data

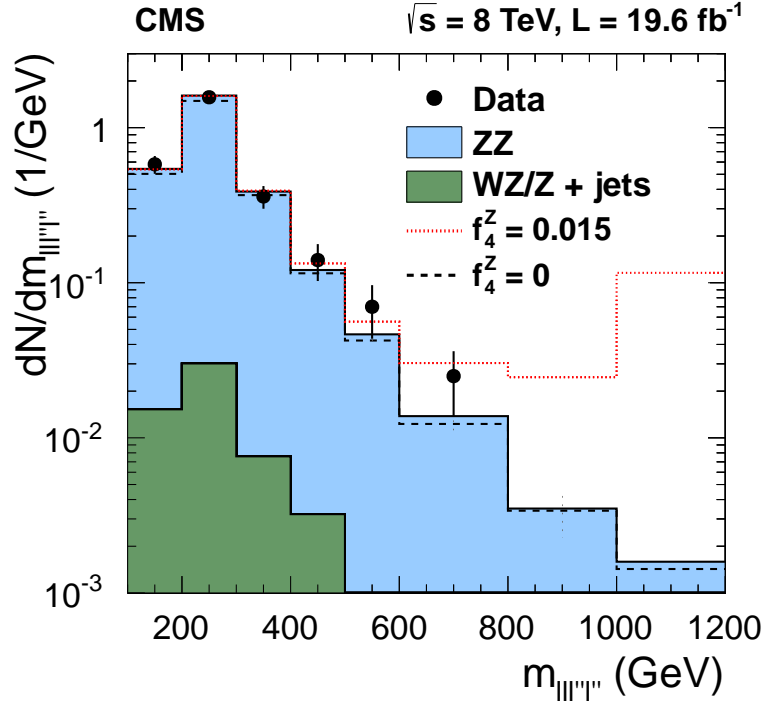


Figure 5: Distribution of the four-lepton reconstructed mass for the combined $4e$, 4μ , and $2e2\mu$ channels. Points represent the data, the shaded histogram labeled ZZ represents the POWHEG+GG2ZZ+PYTHIA predictions for ZZ signal, the histograms labeled WZ/Z+jets shows background, which is estimated from data, as described in the text. The dashed and dotted histograms indicate the results of the SHERPA simulation for the SM ($f_4^Z = 0$) and in the presence of an ATGC ($f_4^Z = 0.015$) with all the other anomalous couplings set to zero. The last bin includes all entries with masses above 1000 GeV.

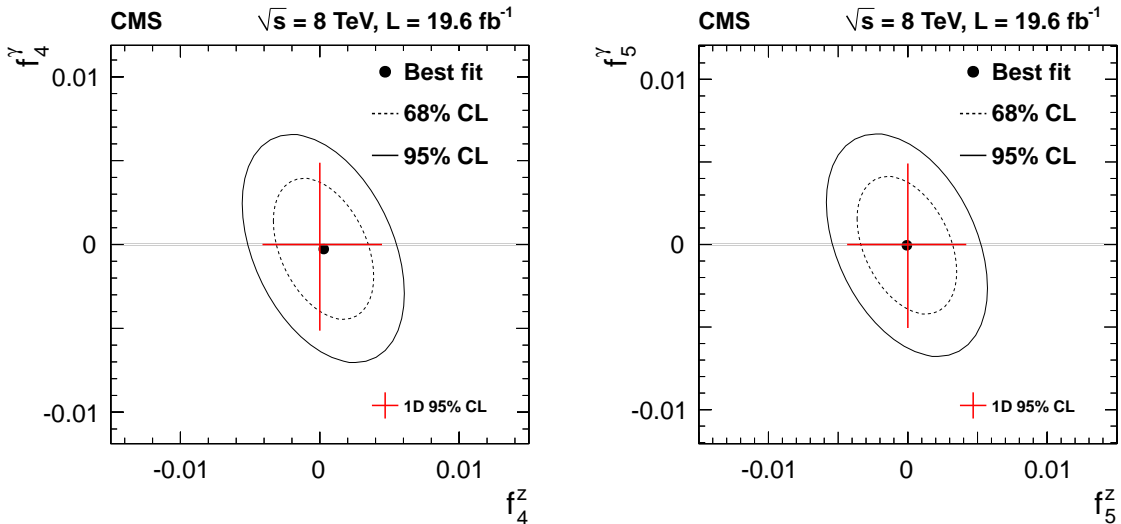


Figure 6: Two-dimensional exclusion limits at 68% (dashed contour) and 95% (solid contour) CL on the ZZZ and ZZ γ ATGCs. The left(right) plot shows the exclusion contour in the $(f_{4(5)}^Z, f_{4(5)}^\gamma)$ parameter planes. The solid dot shows where the likelihood reaches its maximum. The values of couplings outside of contours are excluded at the corresponding confidence level. The lines in the middle represent one-dimensional limits. No form factor is used.

sample corresponds to an integrated luminosity of 19.6 fb^{-1} . The measured total cross section $\sigma(\text{pp} \rightarrow \text{ZZ}) = 7.7 \pm 0.5 \text{ (stat.)}_{-0.4}^{+0.5} \text{ (syst.)} \pm 0.4 \text{ (th.)} \pm 0.2 \text{ (lum.) pb}$ and the differential cross sections agree well with the SM predictions. Improved limits on anomalous ZZZ and $\text{ZZ}\gamma$ triple gauge couplings are established, significantly restricting their possible allowed ranges.

Acknowledgements

We congratulate our colleagues in the CERN accelerator departments for the excellent performance of the LHC and thank the technical and administrative staffs at CERN and at other CMS institutes for their contributions to the success of the CMS effort. In addition, we gratefully acknowledge the computing centres and personnel of the Worldwide LHC Computing Grid for delivering so effectively the computing infrastructure essential to our analyses. Finally, we acknowledge the enduring support for the construction and operation of the LHC and the CMS detector provided by the following funding agencies: BMWFW and FWF (Austria); FNRS and FWO (Belgium); CNPq, CAPES, FAPERJ, and FAPESP (Brazil); MES (Bulgaria); CERN; CAS, MoST, and NSFC (China); COLCIENCIAS (Colombia); MSES and CSF (Croatia); RPF (Cyprus); MoER, ERC IUT and ERDF (Estonia); Academy of Finland, MEC, and HIP (Finland); CEA and CNRS/IN2P3 (France); BMBF, DFG, and HGF (Germany); GSRT (Greece); OTKA and NIH (Hungary); DAE and DST (India); IPM (Iran); SFI (Ireland); INFN (Italy); NRF and WCU (Republic of Korea); LAS (Lithuania); MOE and UM (Malaysia); CINVESTAV, CONACYT, SEP, and UASLP-FAI (Mexico); MBIE (New Zealand); PAEC (Pakistan); MSHE and NSC (Poland); FCT (Portugal); JINR (Dubna); MON, RosAtom, RAS and RFBR (Russia); MESTD (Serbia); SEIDI and CPAN (Spain); Swiss Funding Agencies (Switzerland); MST (Taipei); ThEPCenter, IPST, STAR and NSTDA (Thailand); TUBITAK and TAEK (Turkey); NASU and SFFR (Ukraine); STFC (United Kingdom); DOE and NSF (USA).

Individuals have received support from the Marie-Curie programme and the European Research Council and EPLANET (European Union); the Leventis Foundation; the A. P. Sloan Foundation; the Alexander von Humboldt Foundation; the Belgian Federal Science Policy Office; the Fonds pour la Formation à la Recherche dans l'Industrie et dans l'Agriculture (FRIA-Belgium); the Agentschap voor Innovatie door Wetenschap en Technologie (IWT-Belgium); the Ministry of Education, Youth and Sports (MEYS) of the Czech Republic; the Council of Science and Industrial Research, India; the HOMING PLUS programme of Foundation for Polish Science, cofinanced from European Union, Regional Development Fund; the Compagnia di San Paolo (Torino); and the Thalys and Aristeia programmes cofinanced by EU-ESF and the Greek NSRF.

References

- [1] K. Hagiwara, R. D. Peccei, and D. Zeppenfeld, "Probing the weak boson sector in $e^+e^- \rightarrow W^+W^-$ ", *Nucl. Phys. B* **282** (1987) 253, doi:10.1016/0550-3213(87)90685-7.
- [2] G. J. Gounaris, J. Layssac, and F. M. Renard, "New and standard physics contributions to anomalous Z and gamma self-couplings", *Phys. Rev. D* **62** (2000) 073013, doi:10.1103/PhysRevD.62.073013, arXiv:hep-ph/0003143.
- [3] CMS Collaboration, "Measurement of the ZZ production cross section and search for anomalous couplings in $2\ell 2\ell'$ final states in pp collisions at $\sqrt{s} = 7 \text{ TeV}$ ", *JHEP* **01** (2013) 063, doi:10.1007/JHEP01(2013)063, arXiv:1211.4890.

- [4] CMS Collaboration, “Measurement of W^+W^- and ZZ production cross sections in pp collisions at $\sqrt{s} = 8$ TeV”, *Phys. Lett. B* **721** (2013) 190, doi:10.1016/j.physletb.2013.03.027, arXiv:1301.4698.
- [5] ATLAS Collaboration, “Measurement of ZZ production in pp collisions at $\sqrt{s} = 7$ TeV and limits on anomalous ZZZ and $ZZ\gamma$ couplings with the ATLAS detector”, *JHEP* **03** (2013) 128, doi:10.1007/JHEP03(2013)128, arXiv:1211.6096.
- [6] CDF Collaboration, “Measurement of ZZ production in leptonic final states at \sqrt{s} of 1.96 TeV at CDF”, *Phys. Rev. Lett.* **108** (2012) 101801, doi:10.1103/PhysRevLett.108.101801, arXiv:1112.2978.
- [7] D0 Collaboration, “Measurement of the ZZ production cross section in $p\bar{p}$ collisions at $\sqrt{s} = 1.96$ TeV”, *Phys. Rev. D* **84** (2011) 011103, doi:10.1103/PhysRevD.84.011103, arXiv:1104.3078.
- [8] CMS Collaboration, “The CMS experiment at the CERN LHC”, *JINST* **3** (2008) S08004, doi:10.1088/1748-0221/3/08/S08004.
- [9] S. Alioli, P. Nason, C. Oleari, and E. Re, “NLO vector-boson production matched with shower in POWHEG”, *JHEP* **07** (2008) 060, doi:10.1088/1126-6708/2008/07/060, arXiv:0805.4802.
- [10] P. Nason, “A new method for combining NLO QCD with shower Monte Carlo algorithms”, *JHEP* **11** (2004) 040, doi:10.1088/1126-6708/2004/11/040, arXiv:hep-ph/0409146.
- [11] S. Frixione, P. Nason, and C. Oleari, “Matching NLO QCD computations with parton shower simulations: the POWHEG method”, *JHEP* **11** (2007) 070, doi:10.1088/1126-6708/2007/11/070, arXiv:0709.2092.
- [12] T. Gleisberg et al., “Event generation with SHERPA 1.1”, *JHEP* **02** (2009) 007, doi:10.1088/1126-6708/2009/02/007, arXiv:0811.4622.
- [13] T. Binoth, N. Kauer, and P. Mertsch, “Gluon-induced QCD corrections to $pp \rightarrow ZZ \rightarrow \ell\bar{\ell}\ell'\bar{\ell}'$ ”, (2008). arXiv:0807.0024.
- [14] J. Alwall et al., “MadGraph 5: going beyond”, *JHEP* **06** (2011) 128, doi:10.1007/JHEP06(2011)128, arXiv:1106.0522.
- [15] T. Sjöstrand, S. Mrenna, and P. Z. Skands, “PYTHIA 6.4 physics and manual”, *JHEP* **05** (2006) 026, doi:10.1088/1126-6708/2006/05/026, arXiv:hep-ph/0603175.
- [16] H.-L. Lai et al., “Uncertainty induced by QCD coupling in the CTEQ global analysis of parton distributions”, *Phys. Rev. D* **82** (2010) 054021, doi:10.1103/PhysRevD.82.054021, arXiv:1004.4624.
- [17] H.-L. Lai et al., “New parton distributions for collider physics”, *Phys. Rev. D* **82** (2010) 074024, doi:10.1103/PhysRevD.82.074024, arXiv:1007.2241.
- [18] J. M. Campbell and R. K. Ellis, “MCFM for the Tevatron and the LHC”, *Nucl. Phys. Proc. Suppl.* **205** (2010) 10, doi:10.1016/j.nuclphysbps.2010.08.011, arXiv:1007.3492.

- [19] A. D. Martin, W. J. Stirling, R. S. Thorne, and G. Watt, "Parton distributions for the LHC", *Eur. Phys. J. C* **63** (2009) 189, doi:10.1140/epjc/s10052-009-1072-5, arXiv:0901.0002.
- [20] S. Jadach and Z. Wąs, "The tau decay library TAUOLA: Version 2.4", *Comput. Phys. Commun.* **76** (1993) 361, doi:10.1016/0010-4655(93)90061-G.
- [21] GEANT4 Collaboration, "GEANT4—a simulation toolkit", *Nucl. Instrum. Meth. A* **506** (2003) 250, doi:10.1016/S0168-9002(03)01368-8.
- [22] CMS Collaboration, "Particle-Flow Event Reconstruction in CMS and Performance for Jets, Taus, and E_T^{miss} ", CMS Physics Analysis Summary CMS-PAS-PFT-09-001, 2009.
- [23] CMS Collaboration, "Commissioning of the Particle-flow Event Reconstruction with the first LHC collisions recorded in the CMS detector", CMS Physics Analysis Summary CMS-PAS-PFT-10-001, 2010.
- [24] S. Baffioni et al., "Electron reconstruction in CMS", *Eur. Phys. J. C* **49** (2007) 1099, doi:10.1140/epjc/s10052-006-0175-5.
- [25] W. Adam, R. Fruehwirth, A. Strandlie, and T. Todorov, "Reconstruction of electrons with the Gaussian-sum filter in the CMS tracker at the LHC", *J. Phys. G: Nucl. Part. Phys.* **31** (2005) N9, doi:10.1088/0954-3899/31/9/N01.
- [26] CMS Collaboration, "Performance of CMS muon reconstruction in pp collision events at $\sqrt{s} = 7$ TeV", *JINST* **7** (2012) P10002, doi:10.1088/1748-0221/7/10/P10002, arXiv:1206.4071.
- [27] CMS Collaboration, "Performance of τ -lepton reconstruction and identification in CMS", *JINST* **7** (2012) P01001, doi:10.1088/1748-0221/7/01/P01001.
- [28] M. Cacciari and G. P. Salam, "Pileup subtraction using jet areas", *Phys. Lett. B* **659** (2008) 119, doi:10.1016/j.physletb.2007.09.077, arXiv:0707.1378.
- [29] CMS Collaboration, "Measurement of the Inclusive W and Z Production Cross Sections in pp Collisions at $\sqrt{s} = 7$ TeV", *JHEP* **10** (2011) 132, doi:10.1007/JHEP10(2011)132, arXiv:1107.4789.
- [30] CMS Collaboration, "CMS Luminosity Based on Pixel Cluster Counting – Summer 2013 Update", CMS Physics Analysis Summary CMS-PAS-LUM-13-001, 2013.
- [31] M. Botje et al., "The PDF4LHC Working Group Interim Recommendations", (2011). arXiv:1101.0538.
- [32] D. R. Ball et al., "Impact of Heavy Quark Masses on Parton Distributions and LHC Phenomenology", *Nucl. Phys. B* **849** (2011) 296, doi:10.1016/j.nuclphysb.2011.03.021, arXiv:1101.1300.
- [33] Particle Data Group Collaboration, "Review of Particle Physics", *Phys. Rev. D* **86** (2012) 010001, doi:10.1103/PhysRevD.86.010001.
- [34] G. D'Agostini, "Improved iterative Bayesian unfolding", (2010). arXiv:1010.0632.

10 The CMS Collaboration

Yerevan Physics Institute, Yerevan, Armenia

V. Khachatryan, A.M. Sirunyan, A. Tumasyan

Institut für Hochenergiephysik der OeAW, Wien, Austria

W. Adam, T. Bergauer, M. Dragicevic, J. Erö, C. Fabjan¹, M. Friedl, R. Frühwirth¹, V.M. Ghete, C. Hartl, N. Hörmann, J. Hrubec, M. Jeitler¹, W. Kiesenhofer, V. Knünz, M. Krammer¹, I. Krätschmer, D. Liko, I. Mikulec, D. Rabady², B. Rahbaran, H. Rohringer, R. Schöfbeck, J. Strauss, A. Taurok, W. Treberer-Treberspurg, W. Waltenberger, C.-E. Wulz¹

National Centre for Particle and High Energy Physics, Minsk, Belarus

V. Mossolov, N. Shumeiko, J. Suarez Gonzalez

Universiteit Antwerpen, Antwerpen, Belgium

S. Alderweireldt, M. Bansal, S. Bansal, T. Cornelis, E.A. De Wolf, X. Janssen, A. Knutsson, S. Luyckx, S. Ochesanu, B. Roland, R. Rougny, M. Van De Klundert, H. Van Haevermaet, P. Van Mechelen, N. Van Remortel, A. Van Spilbeeck

Vrije Universiteit Brussel, Brussel, Belgium

F. Blekman, S. Blyweert, J. D'Hondt, N. Daci, N. Heracleous, A. Kalogeropoulos, J. Keaveney, T.J. Kim, S. Lowette, M. Maes, A. Olbrechts, Q. Python, D. Strom, S. Tavernier, W. Van Doninck, P. Van Mulders, G.P. Van Onsem, I. Vilella

Université Libre de Bruxelles, Bruxelles, Belgium

C. Caillol, B. Clerbaux, G. De Lentdecker, D. Dobur, L. Favart, A.P.R. Gay, A. Grebenyuk, A. Léonard, A. Mohammadi, L. Perniè², T. Reis, T. Seva, L. Thomas, C. Vander Velde, P. Vanlaer, J. Wang

Ghent University, Ghent, Belgium

V. Adler, K. Beernaert, L. Benucci, A. Cimmino, S. Costantini, S. Crucy, S. Dildick, A. Fagot, G. Garcia, B. Klein, J. Mccartin, A.A. Ocampo Rios, D. Ryckbosch, S. Salva Diblen, M. Sigamani, N. Strobbe, F. Thyssen, M. Tytgat, E. Yazgan, N. Zaganidis

Université Catholique de Louvain, Louvain-la-Neuve, Belgium

S. Basesmez, C. Beluffi³, G. Bruno, R. Castello, A. Caudron, L. Ceard, G.G. Da Silveira, C. Delaere, T. du Pree, D. Favart, L. Forthomme, A. Giammanco⁴, J. Hollar, P. Jez, M. Komm, V. Lemaître, J. Liao, C. Nuttens, D. Pagano, A. Pin, K. Piotrkowski, A. Popov⁵, L. Quertenmont, M. Selvaggi, M. Vidal Marono, J.M. Vizan Garcia

Université de Mons, Mons, Belgium

N. Bely, T. Caebergs, E. Daubie, G.H. Hammad

Centro Brasileiro de Pesquisas Físicas, Rio de Janeiro, Brazil

G.A. Alves, M. Correa Martins Junior, T. Dos Reis Martins, M.E. Pol

Universidade do Estado do Rio de Janeiro, Rio de Janeiro, Brazil

W.L. Aldá Júnior, W. Carvalho, J. Chinellato⁶, A. Custódio, E.M. Da Costa, D. De Jesus Damiao, C. De Oliveira Martins, S. Fonseca De Souza, H. Malbouisson, M. Malek, D. Matos Figueiredo, L. Mundim, H. Nogima, W.L. Prado Da Silva, J. Santaolalla, A. Santoro, A. Sznajder, E.J. Tonelli Manganote⁶, A. Vilela Pereira

Universidade Estadual Paulista ^a, Universidade Federal do ABC ^b, São Paulo, Brazil

C.A. Bernardes^b, F.A. Dias^{a,7}, T.R. Fernandez Perez Tomei^a, E.M. Gregores^b, P.G. Mercadante^b, S.F. Novaes^a, Sandra S. Padula^a

Institute for Nuclear Research and Nuclear Energy, Sofia, Bulgaria

A. Aleksandrov, V. Genchev², P. Iaydjiev, A. Marinov, S. Piperov, M. Rodozov, G. Sultanov, M. Vutova

University of Sofia, Sofia, Bulgaria

A. Dimitrov, I. Glushkov, R. Hadjiiska, V. Kozhuharov, L. Litov, B. Pavlov, P. Petkov

Institute of High Energy Physics, Beijing, China

J.G. Bian, G.M. Chen, H.S. Chen, M. Chen, R. Du, C.H. Jiang, D. Liang, S. Liang, R. Plestina⁸, J. Tao, X. Wang, Z. Wang

State Key Laboratory of Nuclear Physics and Technology, Peking University, Beijing, China

C. Asawatangtrakuldee, Y. Ban, Y. Guo, Q. Li, W. Li, S. Liu, Y. Mao, S.J. Qian, D. Wang, L. Zhang, W. Zou

Universidad de Los Andes, Bogota, Colombia

C. Avila, L.F. Chaparro Sierra, C. Florez, J.P. Gomez, B. Gomez Moreno, J.C. Sanabria

Technical University of Split, Split, Croatia

N. Godinovic, D. Lelas, D. Polic, I. Puljak

University of Split, Split, Croatia

Z. Antunovic, M. Kovac

Institute Rudjer Boskovic, Zagreb, Croatia

V. Brigljevic, K. Kadija, J. Luetic, D. Mekterovic, L. Sudic

University of Cyprus, Nicosia, Cyprus

A. Attikis, G. Mavromanolakis, J. Mousa, C. Nicolaou, F. Ptochos, P.A. Razis

Charles University, Prague, Czech Republic

M. Bodlak, M. Finger, M. Finger Jr.

Academy of Scientific Research and Technology of the Arab Republic of Egypt, Egyptian Network of High Energy Physics, Cairo, Egypt

Y. Assran⁹, A. Ellithi Kamel¹⁰, M.A. Mahmoud¹¹, A. Radi^{12,13}

National Institute of Chemical Physics and Biophysics, Tallinn, Estonia

M. Kadastik, M. Murumaa, M. Raidal, A. Tiko

Department of Physics, University of Helsinki, Helsinki, Finland

P. Eerola, G. Fedi, M. Voutilainen

Helsinki Institute of Physics, Helsinki, Finland

J. Härkönen, V. Karimäki, R. Kinnunen, M.J. Kortelainen, T. Lampén, K. Lassila-Perini, S. Lehti, T. Lindén, P. Luukka, T. Mäenpää, T. Peltola, E. Tuominen, J. Tuominiemi, E. Tuovinen, L. Wendland

Lappeenranta University of Technology, Lappeenranta, Finland

T. Tuuva

DSM/IRFU, CEA/Saclay, Gif-sur-Yvette, France

M. Besancon, F. Couderc, M. Dejardin, D. Denegri, B. Fabbro, J.L. Faure, C. Favaro, F. Ferri, S. Ganjour, A. Givernaud, P. Gras, G. Hamel de Monchenault, P. Jarry, E. Locci, J. Malcles, A. Nayak, J. Rander, A. Rosowsky, M. Titov

Laboratoire Leprince-Ringuet, Ecole Polytechnique, IN2P3-CNRS, Palaiseau, France

S. Baffioni, F. Beaudette, P. Busson, C. Charlot, T. Dahms, M. Dalchenko, L. Dobrzynski, N. Filipovic, A. Florent, R. Granier de Cassagnac, L. Mastrolorenzo, P. Miné, C. Mironov, I.N. Naranjo, M. Nguyen, C. Ochando, P. Paganini, R. Salerno, J.B. Sauvan, Y. Sirois, C. Veelken, Y. Yilmaz, A. Zabi

Institut Pluridisciplinaire Hubert Curien, Université de Strasbourg, Université de Haute Alsace Mulhouse, CNRS/IN2P3, Strasbourg, France

J.-L. Agram¹⁴, J. Andrea, A. Aubin, D. Bloch, J.-M. Brom, E.C. Chabert, C. Collard, E. Conte¹⁴, J.-C. Fontaine¹⁴, D. Gelé, U. Goerlach, C. Goetzmann, A.-C. Le Bihan, P. Van Hove

Centre de Calcul de l'Institut National de Physique Nucleaire et de Physique des Particules, CNRS/IN2P3, Villeurbanne, France

S. Gadrat

Université de Lyon, Université Claude Bernard Lyon 1, CNRS-IN2P3, Institut de Physique Nucléaire de Lyon, Villeurbanne, France

S. Beauceron, N. Beaupere, G. Boudoul², S. Brochet, C.A. Carrillo Montoya, J. Chasserat, R. Chierici, D. Contardo², P. Depasse, H. El Mamouni, J. Fan, J. Fay, S. Gascon, M. Gouzevitch, B. Ille, T. Kurca, M. Lethuillier, L. Mirabito, S. Perries, J.D. Ruiz Alvarez, D. Sabes, L. Sgandurra, V. Sordini, M. Vander Donckt, P. Verdier, S. Viret, H. Xiao

Institute of High Energy Physics and Informatization, Tbilisi State University, Tbilisi, Georgia

Z. Tsamalaidze¹⁵

RWTH Aachen University, I. Physikalisches Institut, Aachen, Germany

C. Autermann, S. Beranek, M. Bontenackels, B. Calpas, M. Edelhoff, L. Feld, O. Hindrichs, K. Klein, A. Ostapchuk, A. Perieanu, F. Raupach, J. Sammet, S. Schael, D. Sprenger, H. Weber, B. Wittmer, V. Zhukov⁵

RWTH Aachen University, III. Physikalisches Institut A, Aachen, Germany

M. Ata, J. Caudron, E. Dietz-Laursonn, D. Duchardt, M. Erdmann, R. Fischer, A. Güth, T. Hebbeker, C. Heidemann, K. Hoepfner, D. Klingebiel, S. Knutzen, P. Kreuzer, M. Merschmeyer, A. Meyer, M. Olschewski, K. Padeken, P. Papacz, H. Reithler, S.A. Schmitz, L. Sonnenschein, D. Teyssier, S. Thüer, M. Weber

RWTH Aachen University, III. Physikalisches Institut B, Aachen, Germany

V. Cherepanov, Y. Erdogan, G. Flügge, H. Geenen, M. Geisler, W. Haj Ahmad, F. Hoehle, B. Kargoll, T. Kress, Y. Kuessel, J. Lingemann², A. Nowack, I.M. Nugent, L. Perchalla, O. Pooth, A. Stahl

Deutsches Elektronen-Synchrotron, Hamburg, Germany

I. Asin, N. Bartosik, J. Behr, W. Behrenhoff, U. Behrens, A.J. Bell, M. Bergholz¹⁶, A. Bethani, K. Borras, A. Burgmeier, A. Cakir, L. Calligaris, A. Campbell, S. Choudhury, F. Costanza, C. Diez Pardos, S. Dooling, T. Dorland, G. Eckerlin, D. Eckstein, T. Eichhorn, G. Flucke, J. Garay Garcia, A. Geiser, P. Gunnellini, J. Hauk, G. Hellwig, M. Hempel, D. Horton, H. Jung, M. Kasemann, P. Katsas, J. Kieseler, C. Kleinwort, D. Krücker, W. Lange, J. Leonard, K. Lipka, A. Lobanov, W. Lohmann¹⁶, B. Lutz, R. Mankel, I. Marfin, I.-A. Melzer-Pellmann, A.B. Meyer, J. Mnich, A. Mussgiller, S. Naumann-Emme, O. Novgorodova, F. Nowak, E. Ntomari, H. Perrey, D. Pitzl, R. Placakyte, A. Raspereza, P.M. Ribeiro Cipriano, E. Ron, M.Ö. Sahin, J. Salfeld-Nebgen, P. Saxena, R. Schmidt¹⁶, T. Schoerner-Sadenius, M. Schröder, S. Spannagel, A.D.R. Vargas Trevino, R. Walsh, C. Wissing

University of Hamburg, Hamburg, Germany

M. Aldaya Martin, V. Blobel, M. Centis Vignali, J. Erfle, E. Garutti, K. Goebel, M. Görner, M. Gosselink, J. Haller, R.S. Höing, H. Kirschenmann, R. Klanner, R. Kogler, J. Lange, T. Lapsien, T. Lenz, I. Marchesini, J. Ott, T. Peiffer, N. Pietsch, D. Rathjens, C. Sander, H. Schettler, P. Schleper, E. Schlieckau, A. Schmidt, M. Seidel, J. Sibille¹⁷, V. Sola, H. Stadie, G. Steinbrück, D. Troendle, E. Usai, L. Vanelderen

Institut für Experimentelle Kernphysik, Karlsruhe, Germany

C. Barth, C. Baus, J. Berger, C. Böser, E. Butz, T. Chwalek, W. De Boer, A. Descroix, A. Dierlamm, M. Feindt, F. Hartmann², T. Hauth², U. Husemann, I. Katkov⁵, A. Kornmayer², E. Kuznetsova, P. Lobelle Pardo, M.U. Mozer, Th. Müller, A. Nürnberg, G. Quast, K. Rabbertz, F. Ratnikov, S. Röcker, H.J. Simonis, F.M. Stober, R. Ulrich, J. Wagner-Kuhr, S. Wayand, T. Weiler, R. Wolf

Institute of Nuclear and Particle Physics (INPP), NCSR Demokritos, Aghia Paraskevi, Greece

G. Anagnostou, G. Daskalakis, T. Gerasis, V.A. Giakoumopoulou, A. Kyriakis, D. Loukas, A. Markou, C. Markou, A. Psallidas, I. Topsis-Giotis

University of Athens, Athens, Greece

L. Gouskos, A. Panagiotou, N. Saoulidou, E. Stiliaris

University of Ioánnina, Ioánnina, Greece

X. Aslanoglou, I. Evangelou, G. Flouris, C. Foudas, P. Kokkas, N. Manthos, I. Papadopoulos, E. Paradas

Wigner Research Centre for Physics, Budapest, Hungary

G. Bencze, C. Hajdu, P. Hidas, D. Horvath¹⁸, F. Sikler, V. Veszpremi, G. Vesztergombi¹⁹, A.J. Zsigmond

Institute of Nuclear Research ATOMKI, Debrecen, Hungary

N. Beni, S. Czellar, J. Karancsi²⁰, J. Molnar, J. Palinkas, Z. Szillasi

University of Debrecen, Debrecen, Hungary

P. Raics, Z.L. Trocsanyi, B. Ujvari

National Institute of Science Education and Research, Bhubaneswar, India

S.K. Swain

Panjab University, Chandigarh, India

S.B. Beri, V. Bhatnagar, N. Dhingra, R. Gupta, A.K. Kalsi, M. Kaur, M. Mittal, N. Nishu, J.B. Singh

University of Delhi, Delhi, India

Ashok Kumar, Arun Kumar, S. Ahuja, A. Bhardwaj, B.C. Choudhary, A. Kumar, S. Malhotra, M. Naimuddin, K. Ranjan, V. Sharma

Saha Institute of Nuclear Physics, Kolkata, India

S. Banerjee, S. Bhattacharya, K. Chatterjee, S. Dutta, B. Gomber, Sa. Jain, Sh. Jain, R. Khurana, A. Modak, S. Mukherjee, D. Roy, S. Sarkar, M. Sharan

Bhabha Atomic Research Centre, Mumbai, India

A. Abdulsalam, D. Dutta, S. Kailas, V. Kumar, A.K. Mohanty², L.M. Pant, P. Shukla, A. Topkar

Tata Institute of Fundamental Research, Mumbai, India

T. Aziz, S. Banerjee, R.M. Chatterjee, R.K. Dewanjee, S. Dugad, S. Ganguly, S. Ghosh,

M. Guchait, A. Gurtu²¹, G. Kole, S. Kumar, M. Maity²², G. Majumder, K. Mazumdar, G.B. Mohanty, B. Parida, K. Sudhakar, N. Wickramage²³

Institute for Research in Fundamental Sciences (IPM), Tehran, Iran

H. Bakhshiansohi, H. Behnamian, S.M. Etesami²⁴, A. Fahim²⁵, R. Goldouzian, A. Jafari, M. Khakzad, M. Mohammadi Najafabadi, M. Naseri, S. Paktinat Mehdiabadi, B. Safarzadeh²⁶, M. Zeinali

University College Dublin, Dublin, Ireland

M. Felcini, M. Grunewald

INFN Sezione di Bari ^a, Università di Bari ^b, Politecnico di Bari ^c, Bari, Italy

M. Abbrescia^{a,b}, L. Barbone^{a,b}, C. Calabria^{a,b}, S.S. Chhibra^{a,b}, A. Colaleo^a, D. Creanza^{a,c}, N. De Filippis^{a,c}, M. De Palma^{a,b}, L. Fiore^a, G. Iaselli^{a,c}, G. Maggi^{a,c}, M. Maggi^a, S. My^{a,c}, S. Nuzzo^{a,b}, N. Pacifico^a, A. Pompili^{a,b}, G. Pugliese^{a,c}, R. Radogna^{a,b,2}, G. Selvaggi^{a,b}, L. Silvestris^{a,2}, G. Singh^{a,b}, R. Venditti^{a,b}, P. Verwilligen^a, G. Zito^a

INFN Sezione di Bologna ^a, Università di Bologna ^b, Bologna, Italy

G. Abbiendi^a, A.C. Benvenuti^a, D. Bonacorsi^{a,b}, S. Braibant-Giacomelli^{a,b}, L. Brigliadori^{a,b}, R. Campanini^{a,b}, P. Capiluppi^{a,b}, A. Castro^{a,b}, F.R. Cavallo^a, G. Codispoti^{a,b}, M. Cuffiani^{a,b}, G.M. Dallavalle^a, F. Fabbri^a, A. Fanfani^{a,b}, D. Fasanella^{a,b}, P. Giacomelli^a, C. Grandi^a, L. Guiducci^{a,b}, S. Marcellini^a, G. Masetti^{a,2}, A. Montanari^a, F.L. Navarria^{a,b}, A. Perrotta^a, F. Primavera^{a,b}, A.M. Rossi^{a,b}, T. Rovelli^{a,b}, G.P. Siroli^{a,b}, N. Tosi^{a,b}, R. Travaglini^{a,b}

INFN Sezione di Catania ^a, Università di Catania ^b, CSFNSM ^c, Catania, Italy

S. Albergo^{a,b}, G. Cappello^a, M. Chiorboli^{a,b}, S. Costa^{a,b}, F. Giordano^{a,2}, R. Potenza^{a,b}, A. Tricomi^{a,b}, C. Tuve^{a,b}

INFN Sezione di Firenze ^a, Università di Firenze ^b, Firenze, Italy

G. Barbagli^a, V. Ciulli^{a,b}, C. Civinini^a, R. D'Alessandro^{a,b}, E. Focardi^{a,b}, E. Gallo^a, S. Gonzi^{a,b}, V. Gori^{a,b,2}, P. Lenzi^{a,b}, M. Meschini^a, S. Paoletti^a, G. Sguazzoni^a, A. Tropiano^{a,b}

INFN Laboratori Nazionali di Frascati, Frascati, Italy

L. Benussi, S. Bianco, F. Fabbri, D. Piccolo

INFN Sezione di Genova ^a, Università di Genova ^b, Genova, Italy

F. Ferro^a, M. Lo Vetere^{a,b}, E. Robutti^a, S. Tosi^{a,b}

INFN Sezione di Milano-Bicocca ^a, Università di Milano-Bicocca ^b, Milano, Italy

M.E. Dinardo^{a,b}, S. Fiorendi^{a,b,2}, S. Gennai^{a,2}, R. Gerosa², A. Ghezzi^{a,b}, P. Govoni^{a,b}, M.T. Lucchini^{a,b,2}, S. Malvezzi^a, R.A. Manzoni^{a,b}, A. Martelli^{a,b}, B. Marzocchi, D. Menasce^a, L. Moroni^a, M. Paganoni^{a,b}, D. Pedrini^a, S. Ragazzi^{a,b}, N. Redaelli^a, T. Tabarelli de Fatis^{a,b}

INFN Sezione di Napoli ^a, Università di Napoli 'Federico II' ^b, Università della Basilicata (Potenza) ^c, Università G. Marconi (Roma) ^d, Napoli, Italy

S. Buontempo^a, N. Cavallo^{a,c}, S. Di Guida^{a,d,2}, F. Fabozzi^{a,c}, A.O.M. Iorio^{a,b}, L. Lista^a, S. Meola^{a,d,2}, M. Merola^a, P. Paolucci^{a,2}

INFN Sezione di Padova ^a, Università di Padova ^b, Università di Trento (Trento) ^c, Padova, Italy

P. Azzi^a, N. Bacchetta^a, D. Bisello^{a,b}, A. Branca^{a,b}, R. Carlin^{a,b}, P. Checchia^a, M. Dall'Osso^{a,b}, T. Dorigo^a, U. Dosselli^a, M. Galanti^{a,b}, F. Gasparini^{a,b}, U. Gasparini^{a,b}, P. Giubilato^{a,b}, A. Gozzelino^a, K. Kanishchev^{a,c}, S. Lacaprara^a, M. Margoni^{a,b}, J. Pazzini^{a,b}, M. Pegoraro^a, N. Pozzobon^{a,b}, P. Ronchese^{a,b}, F. Simonetto^{a,b}, M. Tosi^{a,b}, A. Triossi^a, S. Ventura^a, A. Zucchetta^{a,b}, G. Zumerle^{a,b}

INFN Sezione di Pavia ^a, Università di Pavia ^b, Pavia, ItalyM. Gabusi^{a,b}, S.P. Ratti^{a,b}, C. Riccardi^{a,b}, P. Salvini^a, P. Vitulo^{a,b}**INFN Sezione di Perugia ^a, Università di Perugia ^b, Perugia, Italy**M. Biasini^{a,b}, G.M. Bilei^a, D. Ciangottini^{a,b}, L. Fanò^{a,b}, P. Lariccia^{a,b}, G. Mantovani^{a,b}, M. Menichelli^a, F. Romeo^{a,b}, A. Saha^a, A. Santocchia^{a,b}, A. Spiezia^{a,b,2}**INFN Sezione di Pisa ^a, Università di Pisa ^b, Scuola Normale Superiore di Pisa ^c, Pisa, Italy**K. Androsov^{a,27}, P. Azzurri^a, G. Bagliesi^a, J. Bernardini^a, T. Boccali^a, G. Broccolo^{a,c}, R. Castaldi^a, M.A. Ciocci^{a,27}, R. Dell'Orso^a, S. Donato^{a,c}, F. Fiori^{a,c}, L. Foà^{a,c}, A. Giassi^a, M.T. Grippo^{a,27}, F. Ligabue^{a,c}, T. Lomtadze^a, L. Martini^{a,b}, A. Messineo^{a,b}, C.S. Moon^{a,28}, F. Palla^{a,2}, A. Rizzi^{a,b}, A. Savoy-Navarro^{a,29}, A.T. Serban^a, P. Spagnolo^a, P. Squillacioti^{a,27}, R. Tenchini^a, G. Tonelli^{a,b}, A. Venturi^a, P.G. Verdini^a, C. Vernieri^{a,c,2}**INFN Sezione di Roma ^a, Università di Roma ^b, Roma, Italy**L. Barone^{a,b}, F. Cavallari^a, D. Del Re^{a,b}, M. Diemoz^a, M. Grassi^{a,b}, C. Jorda^a, E. Longo^{a,b}, F. Margaroli^{a,b}, P. Meridiani^a, F. Micheli^{a,b,2}, S. Nourbakhsh^{a,b}, G. Organtini^{a,b}, R. Paramatti^a, S. Rahatlou^{a,b}, C. Rovelli^a, F. Santanastasio^{a,b}, L. Soffi^{a,b,2}, P. Traczyk^{a,b}**INFN Sezione di Torino ^a, Università di Torino ^b, Università del Piemonte Orientale (Novara) ^c, Torino, Italy**N. Amapane^{a,b}, R. Arcidiacono^{a,c}, S. Argiro^{a,b,2}, M. Arneodo^{a,c}, R. Bellan^{a,b}, C. Biino^a, N. Cartiglia^a, S. Casasso^{a,b,2}, M. Costa^{a,b}, A. Degano^{a,b}, N. Demaria^a, L. Finco^{a,b}, C. Mariotti^a, S. Maselli^a, E. Migliore^{a,b}, V. Monaco^{a,b}, M. Musich^a, M.M. Obertino^{a,c,2}, G. Ortona^{a,b}, L. Pacher^{a,b}, N. Pastrone^a, M. Pelliccioni^a, G.L. Pinna Angioni^{a,b}, A. Potenza^{a,b}, A. Romero^{a,b}, M. Ruspa^{a,c}, R. Sacchi^{a,b}, A. Solano^{a,b}, A. Staiano^a, U. Tamponi^a**INFN Sezione di Trieste ^a, Università di Trieste ^b, Trieste, Italy**S. Belforte^a, V. Candelise^{a,b}, M. Casarsa^a, F. Cossutti^a, G. Della Ricca^{a,b}, B. Gobbo^a, C. La Licata^{a,b}, M. Marone^{a,b}, D. Montanino^{a,b}, A. Schizzi^{a,b,2}, T. Umer^{a,b}, A. Zanetti^a**Kangwon National University, Chunchon, Korea**

S. Chang, A. Kropivnitskaya, S.K. Nam

Kyungpook National University, Daegu, Korea

D.H. Kim, G.N. Kim, M.S. Kim, D.J. Kong, S. Lee, Y.D. Oh, H. Park, A. Sakharov, D.C. Son

Chonnam National University, Institute for Universe and Elementary Particles, Kwangju, Korea

J.Y. Kim, S. Song

Korea University, Seoul, Korea

S. Choi, D. Gyun, B. Hong, M. Jo, H. Kim, Y. Kim, B. Lee, K.S. Lee, S.K. Park, Y. Roh

University of Seoul, Seoul, Korea

M. Choi, J.H. Kim, I.C. Park, S. Park, G. Ryu, M.S. Ryu

Sungkyunkwan University, Suwon, Korea

Y. Choi, Y.K. Choi, J. Goh, E. Kwon, J. Lee, H. Seo, I. Yu

Vilnius University, Vilnius, Lithuania

A. Juodagalvis

National Centre for Particle Physics, Universiti Malaya, Kuala Lumpur, Malaysia

J.R. Komaragiri

Centro de Investigacion y de Estudios Avanzados del IPN, Mexico City, Mexico

H. Castilla-Valdez, E. De La Cruz-Burelo, I. Heredia-de La Cruz³⁰, R. Lopez-Fernandez, A. Sanchez-Hernandez

Universidad Iberoamericana, Mexico City, Mexico

S. Carrillo Moreno, F. Vazquez Valencia

Benemerita Universidad Autonoma de Puebla, Puebla, Mexico

I. Pedraza, H.A. Salazar Ibarguen

Universidad Autónoma de San Luis Potosí, San Luis Potosí, Mexico

E. Casimiro Linares, A. Morelos Pineda

University of Auckland, Auckland, New Zealand

D. Krofcheck

University of Canterbury, Christchurch, New Zealand

P.H. Butler, S. Reucroft

National Centre for Physics, Quaid-I-Azam University, Islamabad, Pakistan

A. Ahmad, M. Ahmad, Q. Hassan, H.R. Hoorani, S. Khalid, W.A. Khan, T. Khurshid, M.A. Shah, M. Shoaib

National Centre for Nuclear Research, Swierk, Poland

H. Bialkowska, M. Bluj, B. Boimska, T. Frueboes, M. Górski, M. Kazana, K. Nawrocki, K. Romanowska-Rybinska, M. Szleper, P. Zalewski

Institute of Experimental Physics, Faculty of Physics, University of Warsaw, Warsaw, Poland

G. Brona, K. Bunkowski, M. Cwiok, W. Dominik, K. Doroba, A. Kalinowski, M. Konecki, J. Krolikowski, M. Misiura, M. Olszewski, W. Wolszczak

Laboratório de Instrumentação e Física Experimental de Partículas, Lisboa, Portugal

P. Bargassa, C. Beirão Da Cruz E Silva, P. Faccioli, P.G. Ferreira Parracho, M. Gallinaro, F. Nguyen, J. Rodrigues Antunes, J. Seixas, J. Varela, P. Vischia

Joint Institute for Nuclear Research, Dubna, Russia

I. Golutvin, V. Karjavin, V. Konoplyanikov, V. Korenkov, G. Kozlov, A. Lanev, A. Malakhov, V. Matveev³¹, V.V. Mitsyn, P. Moisenz, V. Palichik, V. Perelygin, S. Shmatov, S. Shulha, N. Skatchkov, V. Smirnov, E. Tikhonenko, A. Zarubin

Petersburg Nuclear Physics Institute, Gatchina (St. Petersburg), Russia

V. Golovtsov, Y. Ivanov, V. Kim³², P. Levchenko, V. Murzin, V. Oreshkin, I. Smirnov, V. Sulimov, L. Uvarov, S. Vavilov, A. Vorobyev, An. Vorobyev

Institute for Nuclear Research, Moscow, Russia

Yu. Andreev, A. Dermenev, S. Gninenko, N. Golubev, M. Kirsanov, N. Krasnikov, A. Pashenkov, D. Tlisov, A. Toropin

Institute for Theoretical and Experimental Physics, Moscow, Russia

V. Epshteyn, V. Gavrilov, N. Lychkovskaya, V. Popov, G. Safronov, S. Semenov, A. Spiridonov, V. Stolin, E. Vlasov, A. Zhokin

P.N. Lebedev Physical Institute, Moscow, Russia

V. Andreev, M. Azarkin, I. Dremin, M. Kirakosyan, A. Leonidov, G. Mesyats, S.V. Rusakov, A. Vinogradov

Skobeltsyn Institute of Nuclear Physics, Lomonosov Moscow State University, Moscow, Russia

A. Belyaev, E. Boos, V. Bunichev, M. Dubinin⁷, L. Dudko, A. Ershov, V. Klyukhin, O. Kodolova, I. Lokhtin, S. Obraztsov, S. Petrushanko, V. Savrin, A. Snigirev

State Research Center of Russian Federation, Institute for High Energy Physics, Protvino, Russia

I. Azhgirey, I. Bayshev, S. Bitioukov, V. Kachanov, A. Kalinin, D. Konstantinov, V. Krychkin, V. Petrov, R. Ryutin, A. Sobol, L. Tourtchanovitch, S. Troshin, N. Tyurin, A. Uzunian, A. Volkov

University of Belgrade, Faculty of Physics and Vinca Institute of Nuclear Sciences, Belgrade, Serbia

P. Adzic³³, M. Dordevic, M. Ekmedzic, J. Milosevic

Centro de Investigaciones Energéticas Medioambientales y Tecnológicas (CIEMAT), Madrid, Spain

J. Alcaraz Maestre, C. Battilana, E. Calvo, M. Cerrada, M. Chamizo Llatas², N. Colino, B. De La Cruz, A. Delgado Peris, D. Domínguez Vázquez, A. Escalante Del Valle, C. Fernandez Bedoya, J.P. Fernández Ramos, J. Flix, M.C. Fouz, P. Garcia-Abia, O. Gonzalez Lopez, S. Goy Lopez, J.M. Hernandez, M.I. Josa, G. Merino, E. Navarro De Martino, A. Pérez-Calero Yzquierdo, J. Puerta Pelayo, A. Quintario Olmeda, I. Redondo, L. Romero, M.S. Soares

Universidad Autónoma de Madrid, Madrid, Spain

C. Albajar, J.F. de Trocóniz, M. Missiroli

Universidad de Oviedo, Oviedo, Spain

H. Brun, J. Cuevas, J. Fernandez Menendez, S. Folgueras, I. Gonzalez Caballero, L. Lloret Iglesias

Instituto de Física de Cantabria (IFCA), CSIC-Universidad de Cantabria, Santander, Spain

J.A. Brochero Cifuentes, I.J. Cabrillo, A. Calderon, J. Duarte Campderros, M. Fernandez, G. Gomez, A. Graziano, A. Lopez Virto, J. Marco, R. Marco, C. Martinez Rivero, F. Matorras, F.J. Munoz Sanchez, J. Piedra Gomez, T. Rodrigo, A.Y. Rodríguez-Marrero, A. Ruiz-Jimeno, L. Scodellaro, I. Vila, R. Vilar Cortabitarte

CERN, European Organization for Nuclear Research, Geneva, Switzerland

D. Abbaneo, E. Auffray, G. Auzinger, M. Bachtis, P. Baillon, A.H. Ball, D. Barney, A. Benaglia, J. Bendavid, L. Benhabib, J.F. Benitez, C. Bernet⁸, G. Bianchi, P. Bloch, A. Bocci, A. Bonato, O. Bondu, C. Botta, H. Breuker, T. Camporesi, G. Cerminara, T. Christiansen, S. Colafranceschi³⁴, M. D'Alfonso, D. d'Enterria, A. Dabrowski, A. David, F. De Guio, A. De Roeck, S. De Visscher, M. Dobson, N. Dupont-Sagorin, A. Elliott-Peisert, J. Eugster, G. Franzoni, W. Funk, M. Giffels, D. Gigi, K. Gill, D. Giordano, M. Girone, F. Glege, R. Guida, S. Gundacker, M. Guthoff, J. Hammer, M. Hansen, P. Harris, J. Hegeman, V. Innocente, P. Janot, K. Kousouris, K. Krajczar, P. Lecoq, C. Lourenço, N. Magini, L. Malgeri, M. Mannelli, L. Masetti, F. Meijers, S. Mersi, E. Meschi, F. Moortgat, S. Morovic, M. Mulders, P. Musella, L. Orsini, L. Pape, E. Perez, L. Perrozzi, A. Petrilli, G. Petrucciani, A. Pfeiffer, M. Pierini, M. Pimiä, D. Piparo, M. Plagge, A. Racz, G. Rolandi³⁵, M. Rovere, H. Sakulin, C. Schäfer, C. Schwick, S. Sekmen, A. Sharma, P. Siegrist, P. Silva, M. Simon, P. Sphicas³⁶, D. Spiga, J. Steggemann, B. Stieger, M. Stoye, D. Treille, A. Tsiros, G.I. Veres¹⁹, J.R. Vlimant, N. Wardle, H.K. Wöhri, W.D. Zeuner

Paul Scherrer Institut, Villigen, Switzerland

W. Bertl, K. Deiters, W. Erdmann, R. Horisberger, Q. Ingram, H.C. Kaestli, S. König, D. Kotlinski, U. Langenegger, D. Renker, T. Rohe

Institute for Particle Physics, ETH Zurich, Zurich, Switzerland

F. Bachmair, L. Bäni, L. Bianchini, P. Bortignon, M.A. Buchmann, B. Casal, N. Chanon, A. Deisher, G. Dissertori, M. Dittmar, M. Donegà, M. Dünser, P. Eller, C. Grab, D. Hits, W. Lustermann, B. Mangano, A.C. Marini, P. Martinez Ruiz del Arbol, D. Meister, N. Mohr, C. Nägeli³⁷, P. Nef, F. Nessi-Tedaldi, F. Pandolfi, F. Pauss, M. Peruzzi, M. Quittnat, L. Rebane, F.J. Ronga, M. Rossini, A. Starodumov³⁸, M. Takahashi, K. Theofilatos, R. Wallny, H.A. Weber

Universität Zürich, Zurich, Switzerland

C. Amsler³⁹, M.F. Canelli, V. Chiochia, A. De Cosa, A. Hinzmann, T. Hreus, M. Ivova Rikova, B. Kilminster, B. Millan Mejias, J. Ngadiuba, P. Robmann, H. Snoek, S. Taroni, M. Verzetti, Y. Yang

National Central University, Chung-Li, Taiwan

M. Cardaci, K.H. Chen, C. Ferro, C.M. Kuo, W. Lin, Y.J. Lu, R. Volpe, S.S. Yu

National Taiwan University (NTU), Taipei, Taiwan

P. Chang, Y.H. Chang, Y.W. Chang, Y. Chao, K.F. Chen, P.H. Chen, C. Dietz, U. Grundler, W.-S. Hou, K.Y. Kao, Y.J. Lei, Y.F. Liu, R.-S. Lu, D. Majumder, E. Petrakou, X. Shi, Y.M. Tzeng, R. Wilken

Chulalongkorn University, Bangkok, Thailand

B. Asavapibhop, N. Srimanobhas, N. Suwonjandee

Cukurova University, Adana, Turkey

A. Adiguzel, M.N. Bakirci⁴⁰, S. Cerci⁴¹, C. Dozen, I. Dumanoglu, E. Eskut, S. Girgis, G. Gokbulut, E. Gurpinar, I. Hos, E.E. Kangal, A. Kayis Topaksu, G. Onengut⁴², K. Ozdemir, S. Ozturk⁴⁰, A. Polatoz, K. Sogut⁴³, D. Sunar Cerci⁴¹, B. Tali⁴¹, H. Topakli⁴⁰, M. Vergili

Middle East Technical University, Physics Department, Ankara, Turkey

I.V. Akin, B. Bilin, S. Bilmis, H. Gamsizkan, G. Karapinar⁴⁴, K. Ocalan, U.E. Surat, M. Yalvac, M. Zeyrek

Bogazici University, Istanbul, Turkey

E. Gülmez, B. Isildak⁴⁵, M. Kaya⁴⁶, O. Kaya⁴⁶

Istanbul Technical University, Istanbul, Turkey

H. Bahtiyar⁴⁷, E. Barlas, K. Cankocak, F.I. Vardarli, M. Yücel

National Scientific Center, Kharkov Institute of Physics and Technology, Kharkov, Ukraine

L. Levchuk, P. Sorokin

University of Bristol, Bristol, United Kingdom

J.J. Brooke, E. Clement, D. Cussans, H. Flacher, R. Frazier, J. Goldstein, M. Grimes, G.P. Heath, H.F. Heath, J. Jacob, L. Kreczko, C. Lucas, Z. Meng, D.M. Newbold⁴⁸, S. Paramesvaran, A. Poll, S. Senkin, V.J. Smith, T. Williams

Rutherford Appleton Laboratory, Didcot, United Kingdom

K.W. Bell, A. Belyaev⁴⁹, C. Brew, R.M. Brown, D.J.A. Cockerill, J.A. Coughlan, K. Harder, S. Harper, E. Olaiya, D. Petyt, C.H. Shepherd-Themistocleous, A. Thea, I.R. Tomalin, W.J. Womersley, S.D. Worm

Imperial College, London, United Kingdom

M. Baber, R. Bainbridge, O. Buchmuller, D. Burton, D. Colling, N. Cripps, M. Cutajar, P. Dauncey, G. Davies, M. Della Negra, P. Dunne, W. Ferguson, J. Fulcher, D. Futyan, A. Gilbert,

G. Hall, G. Iles, M. Jarvis, G. Karapostoli, M. Kenzie, R. Lane, R. Lucas⁴⁸, L. Lyons, A.-M. Magnan, S. Malik, J. Marrouche, B. Mathias, J. Nash, A. Nikitenko³⁸, J. Pela, M. Pesaresi, K. Petridis, D.M. Raymond, S. Rogerson, A. Rose, C. Seez, P. Sharp[†], A. Tapper, M. Vazquez Acosta, T. Virdee

Brunel University, Uxbridge, United Kingdom

J.E. Cole, P.R. Hobson, A. Khan, P. Kyberd, D. Leggat, D. Leslie, W. Martin, I.D. Reid, P. Symonds, L. Teodorescu, M. Turner

Baylor University, Waco, USA

J. Dittmann, K. Hatakeyama, A. Kasmi, H. Liu, T. Scarborough

The University of Alabama, Tuscaloosa, USA

O. Charaf, S.I. Cooper, C. Henderson, P. Rumerio

Boston University, Boston, USA

A. Avetisyan, T. Bose, C. Fantasia, A. Heister, P. Lawson, C. Richardson, J. Rohlf, D. Sperka, J. St. John, L. Sulak

Brown University, Providence, USA

J. Alimena, S. Bhattacharya, G. Christopher, D. Cutts, Z. Demiragli, A. Ferapontov, A. Garabedian, U. Heintz, S. Jabeen, G. Kukartsev, E. Laird, G. Landsberg, M. Luk, M. Narain, M. Segala, T. Sinthuprasith, T. Speer, J. Swanson

University of California, Davis, Davis, USA

R. Breedon, G. Breto, M. Calderon De La Barca Sanchez, S. Chauhan, M. Chertok, J. Conway, R. Conway, P.T. Cox, R. Erbacher, M. Gardner, W. Ko, R. Lander, T. Miceli, M. Mulhearn, D. Pellett, J. Pilot, F. Ricci-Tam, M. Searle, S. Shalhout, J. Smith, M. Squires, D. Stolp, M. Tripathi, S. Wilbur, R. Yohay

University of California, Los Angeles, USA

R. Cousins, P. Everaerts, C. Farrell, J. Hauser, M. Ignatenko, G. Rakness, E. Takasugi, V. Valuev, M. Weber

University of California, Riverside, Riverside, USA

J. Babb, R. Clare, J. Ellison, J.W. Gary, G. Hanson, J. Heilman, P. Jandir, E. Kennedy, F. Lacroix, H. Liu, O.R. Long, A. Luthra, M. Malberti, H. Nguyen, A. Shrinivas, J. Sturdy, S. Sumowidagdo, S. Wimpenny

University of California, San Diego, La Jolla, USA

W. Andrews, J.G. Branson, G.B. Cerati, S. Cittolin, R.T. D'Agnolo, D. Evans, A. Holzner, R. Kelley, M. Lebourgeois, J. Letts, I. Macneill, D. Olivito, S. Padhi, C. Palmer, M. Pieri, M. Sani, V. Sharma, S. Simon, E. Sudano, M. Tadel, Y. Tu, A. Vartak, F. Würthwein, A. Yagil, J. Yoo

University of California, Santa Barbara, Santa Barbara, USA

D. Barge, J. Bradmiller-Feld, C. Campagnari, T. Danielson, A. Dishaw, K. Flowers, M. Franco Sevilla, P. Geffert, C. George, F. Golf, J. Incandela, C. Justus, N. Mccoll, J. Richman, D. Stuart, W. To, C. West

California Institute of Technology, Pasadena, USA

A. Apresyan, A. Bornheim, J. Bunn, Y. Chen, E. Di Marco, J. Duarte, A. Mott, H.B. Newman, C. Pena, C. Rogan, M. Spiropulu, V. Timciuc, R. Wilkinson, S. Xie, R.Y. Zhu

Carnegie Mellon University, Pittsburgh, USA

V. Azzolini, A. Calamba, R. Carroll, T. Ferguson, Y. Iiyama, M. Paulini, J. Russ, H. Vogel, I. Vorobiev

University of Colorado at Boulder, Boulder, USA

J.P. Cumalat, B.R. Drell, W.T. Ford, A. Gaz, E. Luiggi Lopez, U. Nauenberg, J.G. Smith, K. Stenson, K.A. Ulmer, S.R. Wagner

Cornell University, Ithaca, USA

J. Alexander, A. Chatterjee, J. Chu, S. Dittmer, N. Eggert, W. Hopkins, B. Kreis, N. Mirman, G. Nicolas Kaufman, J.R. Patterson, A. Ryd, E. Salvati, L. Skinnari, W. Sun, W.D. Teo, J. Thom, J. Thompson, J. Tucker, Y. Weng, L. Winstrom, P. Wittich

Fairfield University, Fairfield, USA

D. Winn

Fermi National Accelerator Laboratory, Batavia, USA

S. Abdullin, M. Albrow, J. Anderson, G. Apollinari, L.A.T. Bauerdick, A. Beretvas, J. Berryhill, P.C. Bhat, K. Burkett, J.N. Butler, H.W.K. Cheung, F. Chlebana, S. Cihangir, V.D. Elvira, I. Fisk, J. Freeman, E. Gottschalk, L. Gray, D. Green, S. Grünendahl, O. Gutsche, J. Hanlon, D. Hare, R.M. Harris, J. Hirschauer, B. Hooberman, S. Jindariani, M. Johnson, U. Joshi, K. Kaadze, B. Klima, S. Kwan, J. Linacre, D. Lincoln, R. Lipton, T. Liu, J. Lykken, K. Maeshima, J.M. Marraffino, V.I. Martinez Outschoorn, S. Maruyama, D. Mason, P. McBride, K. Mishra, S. Mrenna, Y. Musienko³¹, S. Nahn, C. Newman-Holmes, V. O'Dell, O. Prokofyev, E. Sexton-Kennedy, S. Sharma, A. Soha, W.J. Spalding, L. Spiegel, L. Taylor, S. Tkaczyk, N.V. Tran, L. Uplegger, E.W. Vaandering, R. Vidal, A. Whitbeck, J. Whitmore, F. Yang

University of Florida, Gainesville, USA

D. Acosta, P. Avery, D. Bourilkov, M. Carver, T. Cheng, D. Curry, S. Das, M. De Gruttola, G.P. Di Giovanni, R.D. Field, M. Fisher, I.K. Furic, J. Hugon, J. Konigsberg, A. Korytov, T. Kypreos, J.F. Low, K. Matchev, P. Milenovic⁵⁰, G. Mitselmakher, L. Muniz, A. Rinkevicius, L. Shchutska, N. Skhirtladze, M. Snowball, J. Yelton, M. Zakaria

Florida International University, Miami, USA

V. Gaultney, S. Hewamanage, S. Linn, P. Markowitz, G. Martinez, J.L. Rodriguez

Florida State University, Tallahassee, USA

T. Adams, A. Askew, J. Bochenek, B. Diamond, J. Haas, S. Hagopian, V. Hagopian, K.F. Johnson, H. Prosper, V. Veeraraghavan, M. Weinberg

Florida Institute of Technology, Melbourne, USA

M.M. Baarmand, M. Hohlmann, H. Kalakhety, F. Yumiceva

University of Illinois at Chicago (UIC), Chicago, USA

M.R. Adams, L. Apanasevich, V.E. Bazterra, D. Berry, R.R. Betts, I. Bucinskaite, R. Cavanaugh, O. Evdokimov, L. Gauthier, C.E. Gerber, D.J. Hofman, S. Khalatyan, P. Kurt, D.H. Moon, C. O'Brien, C. Silkworth, P. Turner, N. Varelas

The University of Iowa, Iowa City, USA

E.A. Albayrak⁴⁷, B. Bilki⁵¹, W. Clarida, K. Dilsiz, F. Duru, M. Haytmyradov, J.-P. Merlo, H. Mermerkaya⁵², A. Mestvirishvili, A. Moeller, J. Nachtman, H. Ogul, Y. Onel, F. Ozok⁴⁷, A. Penzo, R. Rahmat, S. Sen, P. Tan, E. Tiras, J. Wetzel, T. Yetkin⁵³, K. Yi

Johns Hopkins University, Baltimore, USA

B.A. Barnett, B. Blumenfeld, S. Bolognesi, D. Fehling, A.V. Gritsan, P. Maksimovic, C. Martin, M. Swartz

The University of Kansas, Lawrence, USA

P. Baringer, A. Bean, G. Benelli, C. Bruner, J. Gray, R.P. Kenny III, M. Murray, D. Noonan, S. Sanders, J. Sekaric, R. Stringer, Q. Wang, J.S. Wood

Kansas State University, Manhattan, USA

A.F. Barfuss, I. Chakaberia, A. Ivanov, S. Khalil, M. Makouski, Y. Maravin, L.K. Saini, S. Shrestha, I. Svintradze

Lawrence Livermore National Laboratory, Livermore, USA

J. Gronberg, D. Lange, F. Rebassoo, D. Wright

University of Maryland, College Park, USA

A. Baden, B. Calvert, S.C. Eno, J.A. Gomez, N.J. Hadley, R.G. Kellogg, T. Kolberg, Y. Lu, M. Marionneau, A.C. Mignerey, K. Pedro, A. Skuja, M.B. Tonjes, S.C. Tonwar

Massachusetts Institute of Technology, Cambridge, USA

A. Apyan, R. Barbieri, G. Bauer, W. Busza, I.A. Cali, M. Chan, L. Di Matteo, V. Dutta, G. Gomez Ceballos, M. Goncharov, D. Gulhan, M. Klute, Y.S. Lai, Y.-J. Lee, A. Levin, P.D. Luckey, T. Ma, C. Paus, D. Ralph, C. Roland, G. Roland, G.S.F. Stephans, F. Stöckli, K. Sumorok, D. Velicanu, J. Veverka, B. Wyslouch, M. Yang, M. Zanetti, V. Zhukova

University of Minnesota, Minneapolis, USA

B. Dahmes, A. De Benedetti, A. Gude, S.C. Kao, K. Klapoetke, Y. Kubota, J. Mans, N. Pastika, R. Rusack, A. Singovsky, N. Tambe, J. Turkewitz

University of Mississippi, Oxford, USA

J.G. Acosta, S. Oliveros

University of Nebraska-Lincoln, Lincoln, USA

E. Avdeeva, K. Bloom, S. Bose, D.R. Claes, A. Dominguez, R. Gonzalez Suarez, J. Keller, D. Knowlton, I. Kravchenko, J. Lazo-Flores, S. Malik, F. Meier, G.R. Snow

State University of New York at Buffalo, Buffalo, USA

J. Dolen, A. Godshalk, I. Iashvili, A. Kharchilava, A. Kumar, S. Rappoccio

Northeastern University, Boston, USA

G. Alverson, E. Barberis, D. Baumgartel, M. Chasco, J. Haley, A. Massironi, D.M. Morse, D. Nash, T. Orimoto, D. Trocino, D. Wood, J. Zhang

Northwestern University, Evanston, USA

K.A. Hahn, A. Kubik, N. Mucia, N. Odell, B. Pollack, A. Pozdnyakov, M. Schmitt, S. Stoynev, K. Sung, M. Velasco, S. Won

University of Notre Dame, Notre Dame, USA

A. Brinkerhoff, K.M. Chan, A. Drozdetskiy, M. Hildreth, C. Jessop, D.J. Karmgard, N. Kellams, K. Lannon, W. Luo, S. Lynch, N. Marinelli, T. Pearson, M. Planer, R. Ruchti, N. Valls, M. Wayne, M. Wolf, A. Woodard

The Ohio State University, Columbus, USA

L. Antonelli, J. Brinson, B. Bylsma, L.S. Durkin, S. Flowers, C. Hill, R. Hughes, K. Kotov, T.Y. Ling, D. Puigh, M. Rodenburg, G. Smith, C. Vuosalo, B.L. Winer, H. Wolfe, H.W. Wulsin

Princeton University, Princeton, USA

E. Berry, O. Driga, P. Elmer, P. Hebda, A. Hunt, S.A. Koay, P. Lujan, D. Marlow, T. Medvedeva, M. Mooney, J. Olsen, P. Piroué, X. Quan, H. Saka, D. Stickland², C. Tully, J.S. Werner, S.C. Zenz, A. Zuranski

University of Puerto Rico, Mayaguez, USA

E. Brownson, H. Mendez, J.E. Ramirez Vargas

Purdue University, West Lafayette, USA

E. Alagoz, V.E. Barnes, D. Benedetti, G. Bolla, D. Bortoletto, M. De Mattia, A. Everett, Z. Hu, M.K. Jha, M. Jones, K. Jung, M. Kress, N. Leonardo, D. Lopes Pegna, V. Maroussov, P. Merkel, D.H. Miller, N. Neumeister, B.C. Radburn-Smith, I. Shipsey, D. Silvers, A. Svyatkovskiy, F. Wang, W. Xie, L. Xu, H.D. Yoo, J. Zablocki, Y. Zheng

Purdue University Calumet, Hammond, USA

N. Parashar, J. Stupak

Rice University, Houston, USA

A. Adair, B. Akgun, K.M. Ecklund, F.J.M. Geurts, W. Li, B. Michlin, B.P. Padley, R. Redjimi, J. Roberts, J. Zabel

University of Rochester, Rochester, USA

B. Betchart, A. Bodek, R. Covarelli, P. de Barbaro, R. Demina, Y. Eshaq, T. Ferbel, A. Garcia-Bellido, P. Goldenzweig, J. Han, A. Harel, A. Khukhunaishvili, D.C. Miner, G. Petrillo, D. Vishnevskiy

The Rockefeller University, New York, USA

R. Ciesielski, L. Demortier, K. Goulianos, G. Lungu, C. Mesropian

Rutgers, The State University of New Jersey, Piscataway, USA

S. Arora, A. Barker, J.P. Chou, C. Contreras-Campana, E. Contreras-Campana, D. Duggan, D. Ferencek, Y. Gershtein, R. Gray, E. Halkiadakis, D. Hidas, A. Lath, S. Panwalkar, M. Park, R. Patel, V. Rekovic, S. Salur, S. Schnetzer, C. Seitz, S. Somalwar, R. Stone, S. Thomas, P. Thomassen, M. Walker

University of Tennessee, Knoxville, USA

K. Rose, S. Spanier, A. York

Texas A&M University, College Station, USA

O. Bouhali⁵⁴, R. Eusebi, W. Flanagan, J. Gilmore, T. Kamon⁵⁵, V. Khotilovich, V. Krutelyov, R. Montalvo, I. Osipenkov, Y. Pakhotin, A. Perloff, J. Roe, A. Rose, A. Safonov, T. Sakuma, I. Suarez, A. Tatarinov

Texas Tech University, Lubbock, USA

N. Akchurin, C. Cowden, J. Damgov, C. Dragoiu, P.R. Duderu, J. Faulkner, K. Kovitanggoon, S. Kunori, S.W. Lee, T. Libeiro, I. Volobouev

Vanderbilt University, Nashville, USA

E. Appelt, A.G. Delannoy, S. Greene, A. Gurrola, W. Johns, C. Maguire, Y. Mao, A. Melo, M. Sharma, P. Sheldon, B. Snook, S. Tuo, J. Velkovska

University of Virginia, Charlottesville, USA

M.W. Arenton, S. Boutle, B. Cox, B. Francis, J. Goodell, R. Hirosky, A. Ledovskoy, H. Li, C. Lin, C. Neu, J. Wood

Wayne State University, Detroit, USA

S. Gollapinni, R. Harr, P.E. Karchin, C. Kottachchi Kankanamge Don, P. Lamichhane

University of Wisconsin, Madison, USA

D.A. Belknap, D. Carlsmith, M. Cepeda, S. Dasu, S. Duric, E. Friis, R. Hall-Wilton, M. Herndon, A. Hervé, P. Klabbers, J. Klukas, A. Lanaro, C. Lazaridis, A. Levine, R. Loveless, A. Mohapatra, I. Ojalvo, T. Perry, G.A. Pierro, G. Polese, I. Ross, T. Sarangi, A. Savin, W.H. Smith, N. Woods

†: Deceased

1: Also at Vienna University of Technology, Vienna, Austria

2: Also at CERN, European Organization for Nuclear Research, Geneva, Switzerland

3: Also at Institut Pluridisciplinaire Hubert Curien, Université de Strasbourg, Université de Haute Alsace Mulhouse, CNRS/IN2P3, Strasbourg, France

4: Also at National Institute of Chemical Physics and Biophysics, Tallinn, Estonia

5: Also at Skobeltsyn Institute of Nuclear Physics, Lomonosov Moscow State University, Moscow, Russia

6: Also at Universidade Estadual de Campinas, Campinas, Brazil

7: Also at California Institute of Technology, Pasadena, USA

8: Also at Laboratoire Leprince-Ringuet, Ecole Polytechnique, IN2P3-CNRS, Palaiseau, France

9: Also at Suez University, Suez, Egypt

10: Also at Cairo University, Cairo, Egypt

11: Also at Fayoum University, El-Fayoum, Egypt

12: Also at British University in Egypt, Cairo, Egypt

13: Now at Ain Shams University, Cairo, Egypt

14: Also at Université de Haute Alsace, Mulhouse, France

15: Also at Joint Institute for Nuclear Research, Dubna, Russia

16: Also at Brandenburg University of Technology, Cottbus, Germany

17: Also at The University of Kansas, Lawrence, USA

18: Also at Institute of Nuclear Research ATOMKI, Debrecen, Hungary

19: Also at Eötvös Loránd University, Budapest, Hungary

20: Also at University of Debrecen, Debrecen, Hungary

21: Now at King Abdulaziz University, Jeddah, Saudi Arabia

22: Also at University of Visva-Bharati, Santiniketan, India

23: Also at University of Ruhuna, Matara, Sri Lanka

24: Also at Isfahan University of Technology, Isfahan, Iran

25: Also at Sharif University of Technology, Tehran, Iran

26: Also at Plasma Physics Research Center, Science and Research Branch, Islamic Azad University, Tehran, Iran

27: Also at Università degli Studi di Siena, Siena, Italy

28: Also at Centre National de la Recherche Scientifique (CNRS) - IN2P3, Paris, France

29: Also at Purdue University, West Lafayette, USA

30: Also at Universidad Michoacana de San Nicolas de Hidalgo, Morelia, Mexico

31: Also at Institute for Nuclear Research, Moscow, Russia

32: Also at St. Petersburg State Polytechnical University, St. Petersburg, Russia

33: Also at Faculty of Physics, University of Belgrade, Belgrade, Serbia

34: Also at Facoltà Ingegneria, Università di Roma, Roma, Italy

35: Also at Scuola Normale e Sezione dell'INFN, Pisa, Italy

36: Also at University of Athens, Athens, Greece

37: Also at Paul Scherrer Institut, Villigen, Switzerland

38: Also at Institute for Theoretical and Experimental Physics, Moscow, Russia

- 39: Also at Albert Einstein Center for Fundamental Physics, Bern, Switzerland
- 40: Also at Gaziosmanpasa University, Tokat, Turkey
- 41: Also at Adiyaman University, Adiyaman, Turkey
- 42: Also at Cag University, Mersin, Turkey
- 43: Also at Mersin University, Mersin, Turkey
- 44: Also at Izmir Institute of Technology, Izmir, Turkey
- 45: Also at Ozyegin University, Istanbul, Turkey
- 46: Also at Kafkas University, Kars, Turkey
- 47: Also at Mimar Sinan University, Istanbul, Istanbul, Turkey
- 48: Also at Rutherford Appleton Laboratory, Didcot, United Kingdom
- 49: Also at School of Physics and Astronomy, University of Southampton, Southampton, United Kingdom
- 50: Also at University of Belgrade, Faculty of Physics and Vinca Institute of Nuclear Sciences, Belgrade, Serbia
- 51: Also at Argonne National Laboratory, Argonne, USA
- 52: Also at Erzincan University, Erzincan, Turkey
- 53: Also at Yildiz Technical University, Istanbul, Turkey
- 54: Also at Texas A&M University at Qatar, Doha, Qatar
- 55: Also at Kyungpook National University, Daegu, Korea